

Microbiome and metabolome alterations in Nrf2 knockout mice with induced gut inflammation and fed with phenethyl isothiocyanate and cranberry enriched diets

Ran Yin^{1*}, Davit Sargsyan^{1,2,3*}, Renyi Wu^{1*}, Rasika Hudlikar¹, Shanyi Li¹, Hsiao-Chen Kuo^{1,2}, Md Shahid Sarwar^{1,2}, Yuyin Zhou⁴, Zhan Gao⁵, Amy Howell⁶, Chi Chen⁴, Martin J. Blaser⁵ and Ah-Ng Kong^{1*}

¹Department of Pharmaceutics, Ernest Mario School of Pharmacy, Rutgers, The State University of New Jersey, Piscataway, NJ 08854, USA

²Graduate Program in Pharmaceutical Science, Ernest Mario School of Pharmacy, Rutgers, The State University of New Jersey, Piscataway, NJ 08854, USA

³Johnson & Johnson, Translational Medicine and Early Development Statistics, Raritan, NJ, USA

⁴Department of Food Science and Nutrition, University of Minnesota, 1354 St. Paul, MN 55108, USA.

⁵Center for Advanced Biotechnology and Medicine, Rutgers, The State University of New Jersey, Piscataway, NJ, 08854, USA

⁶Rutgers University Marucci Center for Blueberry Cranberry Research, 125A Lake Oswego Road, Chatsworth, NJ 08019

* Equal contribution

Correspondence

Professor Ah-Ng Tony Tong Kong

Rutgers, the State University of New Jersey

Ernest Mario School of Pharmacy, Room 228

160 Frelinghuysen Road, Piscataway, NJ 08854

Phone: +1-848-445-6369/8

Email: kongt@pharmacy.rutgers.edu

Abbreviations

ARE - antioxidant response element
CDCA - chenodeoxycholic acid
DCA - dichloroacetic acid
DSS – dextran sulfate sodium
GCDCA - glycochenodeoxycholic Acid
GDCA - glycodeoxycholic acid
LCA - lithocholic acid
MCA - muricholic acid
NRF2- NF-E2-related factor 2
OTU – operational taxonomic unit
PCA – principal components analysis
PEITC - phenethyl isothiocyanate
qPCR - quantitative polymerase chain reaction

Keywords: microbiome, Nrf2, PEITC, cranberry, DSS

Abstract

Scope

Cranberries are enriched with antioxidants and can help prevent bacterial infections, while phenethyl isothiocyanate (PEITC) found in cruciferous vegetables has anti-cancer and anti-inflammatory properties. Incorporating these into diet may have potential health benefits for human gut. Interactions of microbiome and metabolites with the host's cells play crucial roles in maintaining gastrointestinal (GI) tract balance.

Methods and results

In this study, we focused on the alteration of gut microbiomes and metabolomes by cranberry and PEITC enriched diets in wild-type (WT) and Nrf2 knockout (KO) mice, and the diets' potential in reducing the risk of inflammation. Nrf2 KO mice had higher alpha diversity compared to WT. Cranberry and PEITC limited the inflammatory effect of dextran sulfate sodium (DSS) and increased the diversity of mouse gut microbiota. DSS challenge altered the production of several metabolites while PEITC and cranberry feeding reversed the changes. The enriched diets modulated the metabolic responses to induced inflammation likely via microbial composition alterations. Nrf2 KO mice had lower levels of short-chain fatty acids (SCFA) and amino acids such as glutamate, phenylalanine and proline, and higher levels of secondary bile acids such as dichloroacetic acid (DCA) and lithocholic acid (LCA) that are produced by gut bacteria, and muricholic acid (MCA) that it is a primary bile acid produced by mice including germ-free mice.

Conclusions

Compared to WT, Nrf2 KO mice microbiomes exhibited higher richness and diversity. The results also suggest that PEITC and cranberry-enriched diets positively affected the hosts' microbiomes and increased the production of microbial metabolites. Additionally, the dietary supplements showed the reversal of the negative effect of DSS-induced inflammation on the balance of Firmicutes and Bacteroidetes, the two major phylum in the hosts' intestines. Taken together, this study indicates that the phenotypic expression of Nrf2 impacted the microbiota and metabolic reprogramming induced by DSS-mediated inflammation and dietary supplements of cranberry and PEITC.

1. Introduction

Microbial communities leaving on and in the surfaces of human and animal bodies can drastically affect the host's health. These include archaea, bacteria and fungi that are abundant that inhabit skin and the inner lining of the gastrointestinal tract (GI). (1). They help to metabolize essential nutrients, provide energy and interact with the host's immune system. (2, 3, 4). For example, gut bacteria *Butyricoccus pullicaecorum* and *Butyricoccus pullicaecorum* produce butyrate, an essential metabolite for human GI homeostasis and disease prevention (5). Lactobacillus strains are involved in essential vitamins metabolism (6) and human sleep quality improvement (7). Yet another group of bacterial strains, *bifidobacterium* have been suggested to influence higher cognitive functions in humans and to be associated with depression, pain and brain activity during stress. (8, 9, 10, 11, 12). Numerous studies have been conducted to explore

gut microbiota composition responding to specific conditions such as high fat or high fiber diet, or inflammatory bowel disease (13, 14, 15, 16, 17, 18, 19, 20, 21). In addition, research suggest that host's genotype may influence the human gut microbiota, especially in infancy (22, 23). The combination of host genotype, gut microbiota and postnatal factors such as antibiotic usage, dietary pattern and environmental microbes shows significant influence on human gut development and homeostasis (24, 25). Hence, the underlying mechanism of such microbiota-host crosstalk is crucial but remains poorly understood.

Cranberry have been consumed historically by Native Americans as food and medicine (26). Today, cranberry is widely consumed as fresh and dried fruit, juice and sauce. The berries are known for their high content of proanthocyanidins, flavonoids and other organic acids (27, 28). Cranberry consumption have been associated with reduced risk of urinary tract infections (29, 30) and inflammation (31), and improved cardiovascular health (32).

Phenethyl isothiocyanate (PEITC) belongs to the isothiocyanate family of compounds which are formed when glucosinolates, a class of sulfur-containing compounds found in cruciferous vegetables, are hydrolyzed by myrosinase (33, 34). PEITC has been found to have a wide range of biological activities including anticancer, anti-inflammatory, and antioxidant effects (35, 36).

The composition of the GI microbial communities determines the efficiency of processing food into metabolites including amino acids, bile acids and short-chain fatty acids (SCFA). The current study utilized C57BL/6J wild type (WT) and Nrf2 gene knockout (KO) mice to test diets infused with either cranberry or PEITC. Both food additives have been shown to boost the production of the metabolite production. The health benefits of these additives include cancer prevention and activation of Nrf2 pathway. The latter is a master regulator of oxidative stress and inflammation. The aim of this study was to understand the mechanisms by which cranberry and PEITC can influence the gut microbiome and microbial metabolite production, and further improve the gut health via reducing inflammation and achieving homeostasis.

2. Materials and Methods

2.1 Animals and Study Design

C57BL/6J WT mice were purchased from Jackson Laboratory (Bar Harbor, ME). Our laboratory maintained C57BL/6J Nrf2 KO mice since 2005 (37, 38). Mice were kept in a controlled temperature (20-22°C) and humidity (45–55%) environment under 12-hour light and dark cycles at the Rutgers Animal Facility. Food and water were provided ad libitum. The study consisted of three experiments as shown in Figure 1.

All animals were fed with AIN93M standard grain diet (Research Diets, Inc. NJ) for the first 2 weeks of the experiments to equalize the microbiomes at the baseline. After the equalization period, the mice were randomized to treatment groups.

In the first experiment (Exp01), 18 Nrf2 KO mice were assigned to 2 groups with one group continuing to receive the control diet while 0.05% of PEITC was added to the second group's diet. Further 10 WT mice were randomized into either the control diet or the PEITC-enhanced diet groups in the second experiment (Exp02). Finally, dextran sulfate sodium (DSS) challenge

was introduced to 20 mice to induce gut inflammation, and cranberry-enriched diet added (10% of feed by weight), in the third experiment (Exp03). WT and Nrf2 KO mice were randomized into one of four treatment groups (Naïve, DSS, DSS+PEITC, and DSS+Cranberry) (Figure 1). 2.5% DSS was dissolved in autoclaved water and made freshly weekly. Fecal samples were collected freshly, snap frozen in liquid nitrogen and stored at -80°C for 16S ribosomal RNA (rRNA) sequencing and microbial metabolites analysis. Fecal samples for 16S sequencing were collected at weeks 1 and 5 in Exp01, weeks 0 and 4 in Exp02, and weeks 0, 1 and 8 in Exp03. Additional samples were collected from all mice for metabolomics analysis at weeks 2 and 6 in Exp03. Since the fecal sample collection timing varied slightly between the experiments, it was realigned and labeled as baseline (end of the equalization period, i.e., Week 0), early (weeks 1 through 2) or late (weeks 4 through 8) timepoints.

All animal experiments were conducted under the animal protocol approved by the Institutional Animal Care and Use Committee (IACUC) of Rutgers University.

2.2 16S ribosomal RNA gene sequencing and analysis

PowerSoil DNA Isolation Kit (QIAGEN) was used to extract bacterial DNA from the samples. PCR amplification of the 16S rRNA genes were carried out using PCR primers specific for the V4 region (Supplemental Table 1) (39, 40, 41, 42, 43, 44, 45). Indexed amplicons were pooled and sequenced on *MiSeq* (Illumina) yielding at least 8,000 300 base pair (bp) pair-ended reads. Microbial operational taxonomic units (OTUs) and their taxonomic assignments were analyzed using Quantitative Insights Into Microbial Ecology (QIIME2) bioinformatic pipeline (46, 47) and Divisive Amplicon Denoising Algorithm 2 (DADA2 version 1.16) *R* package (48).

QIIME2 mapped reference at 97% similarity against representative sequences of 97% OTU in SILVA, a high quality rRNA database (49), followed by chimeric sequences removal from subsequent analyses (50). Visualization of the microbiome similarities was performed using the results of principle coordinates analysis (PCoA) on the unweighted unique fraction metric (UniFrac).

DADA2 pipeline was used to process *FastQ* sequence data files containing pair-ended reads with average length of 300 base pairs (bp) into a high-resolution OTU table (i.e., amplicon sequencing variants). The reads were sorted, and quality scores examined, resulting in truncation of forward reads to 280 bp and reverse reads to 220 bp based on the quality score profiles. The reads were then merged and aggregated. Additionally, chimeric OTUs were identified and removed. Taxonomy was assigned to the OTUs by exact matching (100% identity) to SILVA reference database.

OTUs mapped to *Eukaryota* and *Archaea* Kingdoms, as well as OTUs that could not be mapped to a Kingdom, were removed. Additionally, bacterial OTUs belonging to phylum *Cyanobacteria* were removed as contamination from diet. Finally, OTUs not mapped to any bacterial phylum were removed, and the remaining OTUs analyzed.

2.3 Microbial metabolites analysis

The concentrations of microbial metabolites that included free amino acids, bile acids and SCFA were quantified in fecal samples collected at weeks 2 and 6. Liquid chromatography mass

spectrometry (LC-MS)-based targeted analysis was utilized to estimate the metabolite concentrations in the samples (51).

2.4 Statistical Analyses

Shannon diversity index was used to assess alpha diversity in the samples at OTU level. This index can range from zero, which corresponds to having a single class (i.e., a single OTU) in the sample, to $\ln(k)$ with k equally distributed OTUs. Larger values of the index, therefore, represent microbial communities with greater number of and more equally distributed classes (OTUs). The estimates were presented as means +/- standard error of the means (SEM).

Multivariable analysis of variance (ANOVA) was used to estimate the effects of genotype, diet and aging, followed by multiple comparison with false discovery rate (FDR) adjustment for the p-values.

Principal components analysis (PCA) was used to explore bacterial composition of the samples at different taxonomic levels. PCA is a linear transformation that projects the data from the original n -dimensional, correlated space (here, each taxonomic unit was viewed as a dimension) onto a new, orthogonal n -dimensional space such that the first principal component (PC1) is in the direction that explains most of variability in the data, the second (PC2) - the second most and orthogonal to PC1, and so on. The results of the PCA analysis were visualized with biplots by plotting the data against the first two principal components and color-coding the points for genotype, diet or DSS challenge. Simultaneously, the biplots displayed the direction and the magnitude of the original axes (i.e., individual taxonomic units). To assess the predictive power of PCA, multinomial regression on group labels (corresponding to taxonomic units) vs. principal components was performed.

Heatmaps were used to visualize concentrations of metabolites in the samples. The group mean differences were estimated and tested using analysis of variance (ANOVA) for each metabolite individually and presented as boxplots with bars and stars indicating statistically significantly different groups.

3 Results

3.1 Data acquisition

Sequencing depth varied between 30,008 and 422,283 reads per sample (Supplemental Figure 1). Over 94% of OTUs were identified as bacterial. In total, 10,197 (94.78% of total OTUs), 7,994 (98.34%) and 7,558 (96.07%) bacterial OTUs were identified in the 3 experiments respectively (Table 1).

3.2 Diet, genotype and inflammation affect bacterial community richness and diversity

The effect of Nrf2 KO was examined since Nrf2 is a master regulator of anti-oxidative stress and anti-inflammatory responses to external and internal stimuli (52, 53, 54, 55, 56). It was examined by comparing the Nrf2 knockout (KO; -/-) mice with the control, wild type (WT) mice across diets, DSS challenge and aging). Shannon index was used to estimate alpha diversity of the

samples at the out level. The results are presented in Figure 2A. Shannon index average was significantly higher in the Nrf2 KO group compared to WT (p -value < 0.01), and increased as the mice aged, as estimated by a mixed-effects linear regression model. The index averages at both, the early and the late time points were significantly higher than at the baseline (both p -values < 0.01). Alpha diversity was also lower in DSS-challenged groups even when they received the dietary additives of cranberry or PEITC (both p -values < 0.01. Sequencing depth affects Shannon index as higher number of reads increases the probability of observing less common OTUs (Supplemental Figure 2A). Therefore, a sensitivity analysis was conducted to investigate Shannon index inflation due to sequencing depth differences by adding 1 to all OTU counts. This removed Shannon index correlation with sequencing depth (Supplemental Figure 2B). Repeating the analysis of the transformed count data showed that the genotype effect remained significant, with NRF2 KO samples having higher mean Shannon index compared to WT (p -value = 0.02). However, the differences of DSS+cranberry or DSS+PEITC with the unchallenged group became non-significant, with only the DSS+AIN93M group being significantly lower compared to the control (p -value < 0.01). The results are shown in Figure 2B and suggest that the two additives had protective effect on the microbiome richness and diversity. The transformation also removed the aging effect.

3.3 Principal components analysis shows association of microbiome composition with diet and genotype

OTU counts were aggregated at the *Phylum* level. In total, 22 phyla were identified, top 10 of which accounted for >99.96% of all hits. Since deeper sequencing increases chances of identifying rare organisms (Supplemental Figure 3), and the samples varied greatly by sequencing depth (Supplemental Figure 1), rare phylum were excluded from the downstream analysis. Data from the 3 experiments was combined for the analysis, however, each group of samples was visualized separately to highlight the differences between experimental conditions (Figure 4). The PCA suggested relatively high inter-experiment variability, specifically, lower relative abundance of *Bacteroidetes*, and higher relative abundance of *Verrucomicrobia* in Exp03 compared to Exp01 and Exp02. Relative abundances of *Firmicutes* and *Actinobacteria* were higher in the WT DSS-treated mice in the Exp03 compared to all other groups, while *Epsilonbacteraeota* were more abundant in all Nrf2 KO and WT control (AIN93M) groups compared to the rest. DSS+PEITC samples grouped between the negative (no-DSS+ AIN93M) and the positive (DSS+ AIN93M) controls, suggesting protective effect of PEITC on microbiome of DSS-treated mice.

The top 10 most abundant Phylum were used for the PCA. The analysis showed strong effect of diet on the microbial composition. Specifically, relative abundance of *Firmicutes* and *Verrucomicrobia* increased while relative abundance of *Proteobacteria*, *Deferribacteres* and *Epsilonbacteraeota* decreased in all WT DSS-treated groups compared to the control (AIN93M). Exp03 data was reanalyzed separately to remove study effect while examining Nrf2 KO effect (Figure 5).

In total, 31 classes of bacteria were identified across the three experiments. The top classes¹⁷ accounted for more than 99.99% of the total hits. The PCA showed strong negative correlation of

Nrf2 KO with *Bacilli* class (phylum (p.) *Firmicutes*) that was consistent in all 3 experiments (Figure 6). Separately, Exp03 data was reanalyzed, with 18 classes being identified in the samples out of which 16 classes contained almost all of the hits and were used in the analysis. The biplot (Figure 7) showed clear separation by genotype. Relative abundance of *Clostridia* (p. *Firmicutes*) was higher while *Betaproteobacteria*, *Epsilonproteobacteria* and *Deltaproteobacteria* (p. *Proteobacteria*), as well as *Campylobacter* (p. *Epsilonbacteraeota*), *Brachyspirae* (p. *Spirochaetes*), and *Deferrribacteres* (p. *Deferrribacteres*) were lower in the all three DSS-treated groups. *Verrucomicrobiae* (p. *Verrucomicrobia*) and *Gammaproteobacteria* (p. *Proteobacteria*) had higher relative abundance in the DSS+AIN93M and DSS+Cranberry groups.

3.4 Firmicutes/Bacteroidetes ratio

Biological activities such as aging, body mass index change and maintaining intestinal homeostasis have been linked to Firmicutes to Bacteroidetes ratio (F/B) (57, 58). Increased F/B ratio was associated with obesity while the ratio decreased was correlated positively with inflammatory bowel disease (59). Therefore, the F/B ratio was as an endpoint used in this study to examine microbiome composition differences across genotypes, diets and timepoints (Figures 8). The abundance of Firmicutes was lower or equal to the abundance of Bacteroidetes in Exp01 and Exp02 samples but the F/B ratios in the WT mice samples were higher than in the Nrf2 KO samples in all 3 experiments. Mixed-effects linear regression models was used to estimate these differences in Exp03. First, a mixed-effects model with no interaction terms was fitted to the F/B ratios. The F/B ratio averages were significantly lower in DSS+PEITC and DSS+Cranberry groups compared to the AIN93M/no DSS challenge control group ($\log_2[F/B] = -0.51$ and -0.46 , and p-values <0.01 and $=0.01$, respectively). The average ratio was also lower in the Nrf2 KO group compared to WT ($\log_2[F/B] = -1.02$, p-value <0.01). The control group's average F/B ratio difference with the DSS control (DSS+AIN93M) as well as the differences between early or late timepoints vs. baseline were not statistically significant. Next, a genotype-diet interaction term was added to the model. It confirmed the significant association of F/B ratios with genotype ($\log_2[F/B] = -1.40$, p-value <0.01), as well as with PEITC and Cranberry diets ($\log_2[F/B] = -0.60$ and -0.71 , respectively, with both p-values <0.01). Additionally, the F/B ratio of the AIN93M group was significantly lower than the DSS+ AIN93M ($\log_2[F/B] = -1.40$, p-value <0.01). These results suggest that PEITC and Cranberry supplements to the regular grain diet preserved the balance of Firmicutes and Bacteroidetes in the intestines of the hosts treated with DSS.

3.4 Linear Discriminant Analysis of aging and dietary effects

Linear discriminant analysis Effect Size (LEfSe) was conducted in QIIME2 to further examine the effects of aging and diet. The compositional changes in the microbiomes over time were examined by comparing the control samples at baseline (shown in Figure 9A and B in red) with the early (Week 1, Figure 9A in green) and late (Week 4, Figure 9B in green) timepoints. Taxa with relative abundance $\geq 0.1\%$ present in at least one specimen were included. In addition, the cladograms showing the phylogenetic distribution of the microbial lineages associated with different time points, using lineages with Linear Discriminant Analysis (LDA) score ≥ 2.0 were displayed. The analysis showed that *Bacteroidetes Prevotella*, *Bacteroidetes Parabacteroides*,

Bacteroidetes, and *Bacteroidetes S24_7* relative abundance decreased, while *Bacteroidetes Bacteroidales*, *Firmicutes Clostridiales*, *Firmicutes Oscillospira*, *Proteobacteria Desulfovibrionaceae*, and *Tenericutes Anaeroplasma* increased over time.

Separately, the effect of PEITC addition to the diet was examined and presented in figures 9C and D. The figures show the impact of PEITC diet by comparing the microbiota for control diet at baseline (Week 0, shown in red) and at the later timepoints (Weeks 1 or 4, shown in green). Relative abundance of *Firmicutes Ruminococcus* significantly increased and *Bacteroidetes S24_7* significantly decreased at the later time points compared to baseline. Several bacterial taxa were shown to be correlated with diet. Specifically, *Bacteroidetes Odoribacter*, *Tenericutes Mycoplasmataceae* and *Proteobacteria Desulfovibrionaceae* were found in significantly higher abundance while *Firmicutes Clostridiales*, *Firmicutes Ruminococcus* and *Acidobacteria Ellin 6075* abundances were significantly lower in the control diet group compared to the PEITC group.

3.5 Cranberry and PEITC additives partially preserved metabolomic profiles in the DSS-treated mice

Fecal samples of the DSS, DSS+Cranberry and DSS+PEITC treated mice from Exp03 were collected at weeks 2 and 6 and analyzed for the concentrations of free amino acids, bile acids and SCFA.

Principal components analysis was conducted showing that concentrations of all but one (taurine) amino acids were higher in the DSS+Cranberry diet group (Figure 10A). However, for bile acids genotype rather than diet played a bigger role, with higher concentrations of all bile acids, specifically, LCA, DCA, MCA, CDCA, GDCA and GCDCA detected in the Nrf KO compared to WT (Figure 10B).

First few principal components were used as explanatory variables in multinomial regression models to classify the samples by diet, DSS challenge and genotype. The model with the first 3 principal components accurately classified 29 out of 48 samples (60.4%) by diet and DSS challenge, with the predictive power increasing slightly with the addition of PCs (Table 2). To classify the samples by genotype, however, a multinomial model with just PC1 was sufficient to correctly predict the group in 34 out of 48 samples (70.8%) suggesting stronger separation of the samples by genotype (Table 3).

Univariable analysis of metabolite concentrations showed that DSS challenge altered the production of several of them while PEITC and cranberry infused diets protected against the changes (Figure 11A). Specifically, DSS challenge decreased the concentrations of amino acids such as glutamate, phenylalanine, and proline, but the concentration in the PEITC and cranberry fed mouse samples prevented these decreases (Figure 11B-D). PEITC and cranberry cotreatments also reversed the DSS-induced increases of secondary bile acids, mainly deoxycholic acid (DCA), lithocholic acid (LCA), and muricholic acid (MCA) (Figure 11E-G). In contrast, the diet additives had little to no effect on SCFA compared to DSS-challenged mice on regular diet (Figure 11H-J). These results suggest that PEITC and cranberry (rich in

anthocyanins) are capable of modulating the metabolic responses to DSS treatment in the colorectal tract, potentially through their effects on the microbiome.

Lastly, the fecal metabolite concentrations from Nrf2 KO and WT mice samples were compared. Interestingly, the Nrf2 KO mice had lower concentrations of amino acids (shown by glutamate, phenylalanine, and proline) and SCFA, and higher concentrations of secondary bile acids (shown by DCA, LCA, and MCA) compared to the WT mice (Figure 12A-I). These trends mirrored the metabolic profile difference between the DSS-challenged and WT mice.

4 Discussion

The important role of diet and genotype on microbial composition leaving in the host's GI has been systematically reported in the literature.

For example, significant increase of relative abundance of *Firmicutes* (*Clostridiales*, *Lactobacillales*, *Turicibacteriales*) and *Verrucomicrobia* (*Verrucomicrobiales*) has been shown to co-occur with a rapid and consistent dietary response to low fat/high plant polysaccharide, and high fat/sugar diets in gene deficient mice. At the same time, *Bacteroidetes* (*Bacteroidales*) has been shown to decrease significantly in high fat/hi sugar diets. Additionally, dietary shift from low fat/high plant to high fat/high sugar diets significantly altered relative abundances of *Clostridiales* and *Bacteroidales* bacterial orders. Utilizing gnotobiotic mouse model with transplantation of healthy human fecal sample, The low fat/high plant polysaccharide diet also decreased the relative abundance of *Firmicutes Erysipelotrichi*, *Firmicutes Bacilli*, and increased the relative abundance of *Bacteroidetes Bacteroidetes* compared with high fat/high sugar Western diet in gnotobiotic mouse model transplanted with healthy human fecal sample. In a four-week cross over trial, twenty-eight healthy subjects were given 60 g of whole grain barley, brown rice or equal mixture of two ingredients every daily (60). All three whole grain diets significantly increased the gut bacterial diversity, as measured by Shannon's and Simpson's indices They also showed increased relative abundance of phylum *Firmicutes*, while the abundance of *Bacteroidetes* decreased Genus *Bacteroides* was significantly decreased by whole barley and brown rice mix diet but was not affected by either of the single ingredient diet. In addition, genera *Roseburia*, *Bifidobacterium*, *Dialister* and *Odoribacter* were significantly altered only by the whole grain barley diet, and genus *Blautia* by both, mix diet and whole grain barley diet.

Opinions regarding the contribution genotype on human gut microbiota vary due to the potential confounding factors in the studies such as the diet and cultural differences. Simplified animal model in a controlled environment can eliminate the confounding between the genotype and gut microbiota. A 2011 study in mice (61) using automated ribosomal intergenic spacer analysis and length-heterogeneity polymerase chain reaction (L-H PCR) (62) suggested that the observed alterations of microbiome composition were genotype-dependent as all animals were housed at the same facility and given the same diet. Higher dissimilarities between genotypes than sexes were observed suggesting that genotype is a stronger factor than gender in regulating gut microbiota. Another mouse study showed evidence of gut microbiota association with genetic defect of toll-like receptor 2 (TLR2) (63). Genus *Helicobacter* was significantly elevated in

TLR2 knock-out mice compared to the wild type. Additionally, some genetic defect such as NOD2 and ATG16L1 were linked to inflammatory bowel diseases and suggested the host-microbiota interaction by shifting bacterial composition including relative abundance of *Actinobacteria*, *Firmicutes*, and *Proteobacteria*.

The role of gut microbiome has been a focal point of many studies over the past several decades, with its potential beneficial effects in metabolizing essential nutrients, providing energy and enhancing immune system (2, 3, 4). For example, *Butyricicoccus Pullicaecorum* and *Butyricicoccus Pullicaecorum* produce butyrate, an essential metabolite for human homeostasis and disease prevention (5) while *Lactobacillus* strains are involved in essential vitamins metabolism (6). Our study demonstrated that host genotype and diet may alter gut microbiota. Both, bacterial diversity and individual bacterial strain relative abundances changed significantly based on diet and genotype, and Nrf2 KO genotype showed stronger effects on the bacterial diversity than diet. *Firmicutes*, *Bacteroidetes* and *Proteobacteria*, the most abundant bacterial phyla, have been altered by both, diet and Nrf2 KO. Individual bacteria at different taxonomic levels showed a pattern of being consistently affected by both, genotype and diet. For instance, *Firmicutes Ruminococcus* was found in higher relative abundance in the PEITC-added diet groups and in Nrf2 KO mice.

Ruminococcus are anaerobic, gram-positive bacteria and belong to the phylum of *Firmicutes*. So far, eleven *Ruminococcus* species have been identified and fall into bacterial family *Ruminococcaceae* and *Lachnospiraceae* (64, 65). Previous studies showed that *Ruminococcus* degraded and fermented cellulosic biomass into short-chain fatty acid (SCFA) for herbivorous ruminants (66, 67, 68). *Ruminococcus Torques* was reported to be abundant in the irritable bowel syndrome subjects in a placebo control double blind study (69). Multiple probiotic interventions were able to reduce *Ruminococcus Torques* abundance significantly based on results obtained from quantitative real-time polymerase chain reaction (qPCR), suggesting that *Ruminococcus Torques* may be used as biomarker in evaluating probiotic activity. As a part of normal flora in gastrointestinal tract, another *Ruminococcus* species, *Gnavus* showed to be in high abundance in the IBD patients, with increased level of oxidative stress in the gut (70), potentially caused by cytokine production such as TNF-a (71). *Firmicutes* has also been reported to be overpopulated in infants who developed respiratory and skin allergic diseases (72). Mice orally garaged by purified *Ruminococcus Gnavus* also developed airway inflammation by cytokine secretion such as interleukins 25 and 33. This study showed significant increase in the abundance of *Firmicutes Ruminoccus* in fecal samples at the late but not at the early timepoints irrespective of diet and genotype. Aging has been linked to the accumulation of harmful inflammatory bacteria in the guts but in this study, we found that the increased level of *Firmicutes Ruminoccus* was mainly associated with Nrf2 KO suggesting that Nrf2 KO accelerates the increase of *Firmicutes Ruminoccus*'s relative abundance. This suggests that Nrf2 might play an important role in regulating the gut microbiota profile and suppress pathogenic species such as *Firmicutes Ruminoccus* as the animal age.

Interestingly, we also observed that the phylum *Ruminococcus* were elevated at the early timepoint in the PEITC groups. *Bacteroidetes Rikenella* was also found significantly elevated in Nrf2 KO

groups, suggesting that it may correlate with gut diseases (73, 74, 75, 76). Overall, genetic KO (mutation) has a strong impact on the host microbiota profile over time and should be considered as a biomarker when developing probiotic or microbiota intervention therapy in the future.

The current study suggests a strong association of mice genotype with gut microbiome richness, diversity and composition. However, a number of factors might have contributed to some of the observed variability. In a mouse study, the cage effect, i.e., housing arrangement of the animals, and individual mouse-to-mouse differences were attributed to explain up to 32% and 46% of gut microbiome composition variability, respectively (77). Possible ways to reduce the background noise in these studies include equalizing the microbiomes at baseline by feeding the animals with a control diet for several weeks or using gnotobiotic (germ-free) mice implanted with homogenized fecal samples (78, 79, 80). We employed the former approach in this study but the amount of variability at the baseline was still noteworthy. Gnotobiotic models typically result in much more homogeneous microbiomes at the baseline, but they are not without complications as they require germ-free facilities and the animals' immune system may be affected by the lack of microbiome at the early stages of their lives. A good compromise is the use of animals pretreated with wide-spectrum antibiotics and provided with high fiber content food before implanting them with homogenized fecal samples (81).

5 Acknowledgment

6 Conflict of Interests

The authors declare no conflicts of interest.

7 Autor Contribution

All authors with (*) contributed significantly to this manuscript.

8 References

1. Dethlefsen L, McFall-Ngai M, Relman DA. An ecological and evolutionary perspective on human-microbe mutualism and disease. *Nature*. 2007;449(7164):811-8.
2. Ramakrishna BS. Role of the gut microbiota in human nutrition and metabolism. *J Gastroen Hepatol*. 2013;28:9-17.
3. Rowland I, Gibson G, Heinken A, Scott K, Swann J, Thiele I, et al. Gut microbiota functions: metabolism of nutrients and other food components. *Eur J Nutr*. 2018;57(1):1-24.
4. Maslowski KM, Mackay CR. Diet, gut microbiota and immune responses. *Nat Immunol*. 2011;12(1):5-9.
5. Geirnaert A, Calatayud M, Grootaert C, Laukens D, Devriese S, Smagghe G, et al. Butyrate-producing bacteria supplemented in vitro to Crohn's disease patient microbiota increased butyrate production and enhanced intestinal epithelial barrier integrity. *Sci Rep-Uk*. 2017;7.
6. LeBlanc JG, Milani C, de Giori GS, Sesma F, van Sinderen D, Ventura M. Bacteria as vitamin suppliers to their host: a gut microbiota perspective. *Curr Opin Biotech*. 2013;24(2):160-8.
7. Aizawa E, Tsuji H, Asahara T, Takahashi T, Teraishi T, Yoshida S, et al. Bifidobacterium and Lactobacillus Counts in the Gut Microbiota of Patients With Bipolar Disorder and Healthy Controls. *Front Psychiatry*. 2018;9:730.

8. Desbonnet L, Garrett L, Clarke G, Kiely B, Cryan JF, Dinan TG. Effects of the Probiotic *Bifidobacterium Infantis* in the Maternal Separation Model of Depression. *Neuroscience*. 2010;170(4):1179-88.
9. Schmidt C. Mental health: thinking from the gut. *Nature*. 2015;518(7540):S12-5.
10. Tillisch K, Labus JS, Ebrat B, Stains J, Naliboff BD, Guyonnet D, et al. Modulation of the Brain-Gut Axis After 4-Week Intervention With a Probiotic Fermented Dairy Product. *Gastroenterology*. 2012;142(5):S115-S.
11. Cryan JF, Dinan TG. Mind-altering microorganisms: the impact of the gut microbiota on brain and behaviour. *Nat Rev Neurosci*. 2012;13(10):701-12.
12. McKernan DP, Fitzgerald P, Dinan TG, Cryan JF. The probiotic *Bifidobacterium infantis* 35624 displays visceral antinociceptive effects in the rat. *Neurogastroent Motil*. 2010;22(9):1029-+.
13. Cani PD, Bibiloni R, Knauf C, Waget A, Neyrinck AM, Delzenne NM, et al. Changes in gut microbiota control metabolic endotoxemia-induced inflammation in high-fat diet-induced obesity and diabetes in mice. *Diabetes*. 2008;57(6):1470-81.
14. Kim KA, Gu W, Lee IA, Joh EH, Kim DH. High fat diet-induced gut microbiota exacerbates inflammation and obesity in mice via the TLR4 signaling pathway. *PLoS One*. 2012;7(10):e47713.
15. Daniel H, Gholami AM, Berry D, Desmarchelier C, Hahne H, Loh G, et al. High-fat diet alters gut microbiota physiology in mice. *ISME J*. 2014;8(2):295-308.
16. Shim JO. Gut microbiota in inflammatory bowel disease. *Pediatr Gastroenterol Hepatol Nutr*. 2013;16(1):17-21.
17. Eom T, Kim YS, Choi CH, Sadowsky MJ, Unno T. Current understanding of microbiota- and dietary-therapies for treating inflammatory bowel disease. *J Microbiol*. 2018;56(3):189-98.
18. Butel MJ. Probiotics, gut microbiota and health. *Med Maladies Infect*. 2014;44(1):1-8.
19. Sekirov I, Russell SL, Antunes LCM, Finlay BB. Gut Microbiota in Health and Disease. *Physiol Rev*. 2010;90(3):859-904.
20. Chen L, Liu B, Ren L, Du H, Fei C, Qian C, et al. High-fiber diet ameliorates gut microbiota, serum metabolism and emotional mood in type 2 diabetes patients. *Front Cell Infect Microbiol*. 2023;13:1069954.
21. Heinritz SN, Weiss E, Eklund M, Aumiller T, Louis S, Rings A, et al. Intestinal Microbiota and Microbial Metabolites Are Changed in a Pig Model Fed a High-Fat/Low-Fiber or a Low-Fat/High-Fiber Diet. *PLoS One*. 2016;11(4):e0154329.
22. Spor A, Koren O, Ley R. Unravelling the effects of the environment and host genotype on the gut microbiome. *Nat Rev Microbiol*. 2011;9(4):279-90.
23. Olivares M, Laparra JM, Sanz Y. Host genotype, intestinal microbiota and inflammatory disorders. *Br J Nutr*. 2013;109 Suppl 2:S76-80.
24. Carmody RN, Gerber GK, Luevano JM, Jr., Gatti DM, Somes L, Svenson KL, et al. Diet dominates host genotype in shaping the murine gut microbiota. *Cell Host Microbe*. 2015;17(1):72-84.
25. Ussar S, Griffin NW, Bezy O, Fujisaka S, Vienberg S, Softic S, et al. Interactions between Gut Microbiota, Host Genetics and Diet Modulate the Predisposition to Obesity and Metabolic Syndrome. *Cell Metab*. 2015;22(3):516-30.
26. Neto CC, Vinson JA. Cranberry. In: Benzie IFF, Wachtel-Galor S, editors. *Herbal Medicine: Biomolecular and Clinical Aspects*. 2nd ed. Boca Raton (FL)2011.
27. Feghali K, Feldman M, La VD, Santos J, Grenier D. Cranberry proanthocyanidins: natural weapons against periodontal diseases. *J Agric Food Chem*. 2012;60(23):5728-35.
28. Wang Y, Johnson-Cicalese J, Singh AP, Vorsa N. Characterization and quantification of flavonoids and organic acids over fruit development in American cranberry (*Vaccinium macrocarpon*) cultivars using HPLC and APCI-MS/MS. *Plant Sci*. 2017;262:91-102.

29. Jepson RG, Williams G, Craig JC. Cranberries for preventing urinary tract infections. *Cochrane Database Syst Rev.* 2012;10(10):CD001321.
30. Howell AB. Bioactive compounds in cranberries and their role in prevention of urinary tract infections. *Mol Nutr Food Res.* 2007;51(6):732-7.
31. Cai X, Han Y, Gu M, Song M, Wu X, Li Z, et al. Dietary cranberry suppressed colonic inflammation and alleviated gut microbiota dysbiosis in dextran sodium sulfate-treated mice. *Food Funct.* 2019;10(10):6331-41.
32. Reed J. Cranberry flavonoids, atherosclerosis and cardiovascular health. *Crit Rev Food Sci Nutr.* 2002;42(3 Suppl):301-16.
33. Johnson IT. Glucosinolates: bioavailability and importance to health. *Int J Vitam Nutr Res.* 2002;72(1):26-31.
34. Dayalan Naidu S, Suzuki T, Yamamoto M, Fahey JW, Dinkova-Kostova AT. Phenethyl Isothiocyanate, a Dual Activator of Transcription Factors NRF2 and HSF1. *Mol Nutr Food Res.* 2018;62(18):e1700908.
35. Gupta P, Wright SE, Kim SH, Srivastava SK. Phenethyl isothiocyanate: a comprehensive review of anti-cancer mechanisms. *Biochim Biophys Acta.* 2014;1846(2):405-24.
36. Keum YS, Owuor ED, Kim BR, Hu R, Kong AN. Involvement of Nrf2 and JNK1 in the activation of antioxidant responsive element (ARE) by chemopreventive agent phenethyl isothiocyanate (PEITC). *Pharm Res.* 2003;20(9):1351-6.
37. Shen G, Xu C, Hu R, Jain MR, Gopalkrishnan A, Nair S, et al. Modulation of nuclear factor E2-related factor 2-mediated gene expression in mice liver and small intestine by cancer chemopreventive agent curcumin. *Mol Cancer Ther.* 2006;5(1):39-51.
38. Lin W, Wu RT, Wu TY, Khor TO, Wang H, Kong AN. Sulforaphane suppressed LPS-induced inflammation in mouse peritoneal macrophages through Nrf2 dependent pathway. *Biochem Pharmacol.* 2008;76(8):967-73.
39. Apprill A, McNally S, Parsons R, Weber L. Minor revision to V4 region SSU rRNA 806R gene primer greatly increases detection of SAR11 bacterioplankton. *Aquat Microb Ecol.* 2015;75(2):129-37.
40. Caporaso JG, Lauber CL, Walters WA, Berg-Lyons D, Lozupone CA, Turnbaugh PJ, et al. Global patterns of 16S rRNA diversity at a depth of millions of sequences per sample. *P Natl Acad Sci USA.* 2011;108:4516-22.
41. Caporaso JG, Lauber CL, Walters WA, Berg-Lyons D, Huntley J, Fierer N, et al. Ultra-high-throughput microbial community analysis on the Illumina HiSeq and MiSeq platforms. *Isme J.* 2012;6(8):1621-4.
42. Minich JJ, Humphrey G, Benitez RAS, Sanders J, Swofford A, Allen EE, et al. High-Throughput Miniaturized 16S rRNA Amplicon Library Preparation Reduces Costs while Preserving Microbiome Integrity. *Msystems.* 2018;3(6).
43. Parada AE, Needham DM, Fuhrman JA. Every base matters: assessing small subunit rRNA primers for marine microbiomes with mock communities, time series and global field samples. *Environ Microbiol.* 2016;18(5):1403-14.
44. Quince C, Lanzen A, Davenport RJ, Turnbaugh PJ. Removing Noise From Pyrosequenced Amplicons. *Bmc Bioinformatics.* 2011;12.
45. Walters W, Hyde ER, Berg-Lyons D, Ackermann G, Humphrey G, Parada A, et al. Improved Bacterial 16S rRNA Gene (V4 and V4-5) and Fungal Internal Transcribed Spacer Marker Gene Primers for Microbial Community Surveys. *Msystems.* 2016;1(1).
46. Bolyen E, Rideout JR, Dillon MR, Bokulich NA, Abnet CC, Al-Ghalith GA, et al. Reproducible, interactive, scalable and extensible microbiome data science using QIIME 2. *Nat Biotechnol.* 2019;37(8):852-7.

47. Estaki M, Jiang L, Bokulich NA, McDonald D, Gonzalez A, Kosciolek T, et al. QIIME 2 Enables Comprehensive End-to-End Analysis of Diverse Microbiome Data and Comparative Studies with Publicly Available Data. *Curr Protoc Bioinformatics*. 2020;70(1):e100.
48. Callahan BJ, McMurdie PJ, Rosen MJ, Han AW, Johnson AJ, Holmes SP. DADA2: High-resolution sample inference from Illumina amplicon data. *Nat Methods*. 2016;13(7):581-3.
49. Yilmaz P, Parfrey LW, Yarza P, Gerken J, Pruesse E, Quast C, et al. The SILVA and "All-species Living Tree Project (LTP)" taxonomic frameworks. *Nucleic Acids Research*. 2014;42(D1):D643-D8.
50. Caporaso JG, Kuczynski J, Stombaugh J, Bittinger K, Bushman FD, Costello EK, et al. QIIME allows analysis of high-throughput community sequencing data. *Nat Methods*. 2010;7(5):335-6.
51. Hung YT, Song Y, Hu Q, Faris RJ, Guo J, Ma Y, et al. Identification of Independent and Shared Metabolic Responses to High-Fiber and Antibiotic Treatments in Fecal Metabolome of Grow-Finish Pigs. *Metabolites*. 2022;12(8).
52. Huang Y, Li W, Su ZY, Kong AN. The complexity of the Nrf2 pathway: beyond the antioxidant response. *J Nutr Biochem*. 2015;26(12):1401-13.
53. Zhang DD. Mechanistic studies of the Nrf2-Keap1 signaling pathway. *Drug Metab Rev*. 2006;38(4):769-89.
54. Taguchi K, Yamamoto M. The KEAP1-NRF2 System in Cancer. *Front Oncol*. 2017;7:85.
55. Mitsuishi Y, Motohashi H, Yamamoto M. The Keap1-Nrf2 system in cancers: stress response and anabolic metabolism. *Front Oncol*. 2012;2:200.
56. Osburn WO, Kensler TW. Nrf2 signaling: an adaptive response pathway for protection against environmental toxic insults. *Mutat Res*. 2008;659(1-2):31-9.
57. Mariat D, Firmesse O, Levenez F, Guimaraes V, Sokol H, Dore J, et al. The Firmicutes/Bacteroidetes ratio of the human microbiota changes with age. *BMC Microbiol*. 2009;9:123.
58. Koliada A, Syzenko G, Moseiko V, Budovska L, Puchkov K, Perederiy V, et al. Association between body mass index and Firmicutes/Bacteroidetes ratio in an adult Ukrainian population. *BMC Microbiol*. 2017;17(1):120.
59. Stojanov S, Berlec A, Strukelj B. The Influence of Probiotics on the Firmicutes/Bacteroidetes Ratio in the Treatment of Obesity and Inflammatory Bowel disease. *Microorganisms*. 2020;8(11).
60. Martinez I, Lattimer JM, Hubach KL, Case JA, Yang JY, Weber CG, et al. Gut microbiome composition is linked to whole grain-induced immunological improvements. *Isme J*. 2013;7(2):269-80.
61. Kovacs A, Ben-Jacob N, Tayem H, Halperin E, Iraqi FA, Gophna U. Genotype Is a Stronger Determinant than Sex of the Mouse Gut Microbiota. *Microb Ecol*. 2011;61(2):423-8.
62. Ritchie NJ, Schutter ME, Dick RP, Myrold DD. Use of length heterogeneity PCR and fatty acid methyl ester profiles to characterize microbial communities in soil. *Appl Environ Microbiol*. 2000;66(4):1668-75.
63. Albert EJ, Sommerfeld K, Gophna S, Marshall JS, Gophna U. The gut microbiota of toll-like receptor 2-deficient mice exhibits lineage-specific modifications. *Environ Microbiol Rep*. 2009;1(1):65-70.
64. La Reau AJ, Suen G. The Ruminococci: key symbionts of the gut ecosystem. *J Microbiol*. 2018;56(3):199-208.
65. Rainey FA, Janssen PH. Phylogenetic analysis by 16S ribosomal DNA sequence comparison reveals two unrelated groups of species within the genus Ruminococcus. *FEMS Microbiol Lett*. 1995;129(1):69-73.
66. Qin J, Li R, Raes J, Arumugam M, Burgdorf KS, Manichanh C, et al. A human gut microbial gene catalogue established by metagenomic sequencing. *Nature*. 2010;464(7285):59-65.
67. Leschine SB. Cellulose degradation in anaerobic environments. *Annu Rev Microbiol*. 1995;49:399-426.

68. Flint HJ, Bayer EA, Rincon MT, Lamed R, White BA. Polysaccharide utilization by gut bacteria: potential for new insights from genomic analysis. *Nat Rev Microbiol.* 2008;6(2):121-31.
69. Lyra A, Krogius-Kurikka L, Nikkila J, Malinen E, Kajander K, Kurikka K, et al. Effect of a multispecies probiotic supplement on quantity of irritable bowel syndrome-related intestinal microbial phylotypes. *BMC Gastroenterol.* 2010;10:110.
70. Hall AB, Yassour M, Sauk J, Garner A, Jiang X, Arthur T, et al. A novel *Ruminococcus gnavus* clade enriched in inflammatory bowel disease patients. *Genome Med.* 2017;9(1):103.
71. Henke MT, Kenny DJ, Cassilly CD, Vlamakis H, Xavier RJ, Clardy J. *Ruminococcus gnavus*, a member of the human gut microbiome associated with Crohn's disease, produces an inflammatory polysaccharide. *Proc Natl Acad Sci U S A.* 2019;116(26):12672-7.
72. Chua HH, Chou HC, Tung YL, Chiang BL, Liao CC, Liu HH, et al. Intestinal Dysbiosis Featuring Abundance of *Ruminococcus gnavus* Associates With Allergic Diseases in Infants. *Gastroenterology.* 2018;154(1):154-67.
73. Johnson EL, Heaver SL, Walters WA, Ley RE. Microbiome and metabolic disease: revisiting the bacterial phylum Bacteroidetes. *J Mol Med (Berl).* 2017;95(1):1-8.
74. Couturier-Maillard A, Secher T, Rehman A, Normand S, De Arcangelis A, Haesler R, et al. NOD2-mediated dysbiosis predisposes mice to transmissible colitis and colorectal cancer. *J Clin Invest.* 2013;123(2):700-11.
75. Carmichael WW. Cyanobacteria secondary metabolites--the cyanotoxins. *J Appl Bacteriol.* 1992;72(6):445-59.
76. Carmichael WW. The toxins of cyanobacteria. *Sci Am.* 1994;270(1):78-86.
77. Hildebrand F, Nguyen TL, Brinkman B, Yunta RG, Cauwe B, Vandenebeele P, et al. Inflammation-associated enterotypes, host genotype, cage and inter-individual effects drive gut microbiota variation in common laboratory mice. *Genome Biol.* 2013;14(1):R4.
78. Roopchand DE, Carmody RN, Kuhn P, Moskal K, Rojas-Silva P, Turnbaugh PJ, et al. Dietary Polyphenols Promote Growth of the Gut Bacterium *Akkermansia muciniphila* and Attenuate High-Fat Diet-Induced Metabolic Syndrome. *Diabetes.* 2015;64(8):2847-58.
79. Zhang L, Carmody RN, Kalariya HM, Duran RM, Moskal K, Poulev A, et al. Grape proanthocyanidin-induced intestinal bloom of *Akkermansia muciniphila* is dependent on its baseline abundance and precedes activation of host genes related to metabolic health. *J Nutr Biochem.* 2018;56:142-51.
80. Turnbaugh PJ, Ridaura VK, Faith JJ, Rey FE, Knight R, Gordon JI. The effect of diet on the human gut microbiome: a metagenomic analysis in humanized gnotobiotic mice. *Sci Transl Med.* 2009;1(6):6ra14.
81. Lundberg R, Toft MF, August B, Hansen AK, Hansen CH. Antibiotic-treated versus germ-free rodents for microbiota transplantation studies. *Gut Microbes.* 2016;7(1):68-74.

Experiment 1:

Group1: Nrf2^{-/-}, AIN93M (N=9)

Group2: Nrf2^{-/-}, PEITC (N=9)

Experiment 2:

Group3: WT, AIN93M (N=5)

Group4: WT, PEITC (N=5)

Experiment 3:

Group5: WT, AIN93M (N=5)

Group6: WT, AIN93M, DSS (N=5)

Group7: WT, Cranberry, DSS (N=5)

Group8: WT, PEITC, DSS (N=5)

Group9: Nrf2^{-/-}, AIN93M (N=5)

Group10: Nrf2^{-/-}, AIN93M, DSS (N=5)

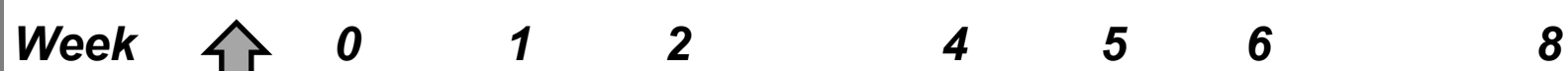
Group11: Nrf2^{-/-}, Cranberry, DSS (N=5)

Group12: Nrf2^{-/-}, PEITC, DSS (N=5)

AIN93M : Groups 1, 3, 5, 6, 9 and 10

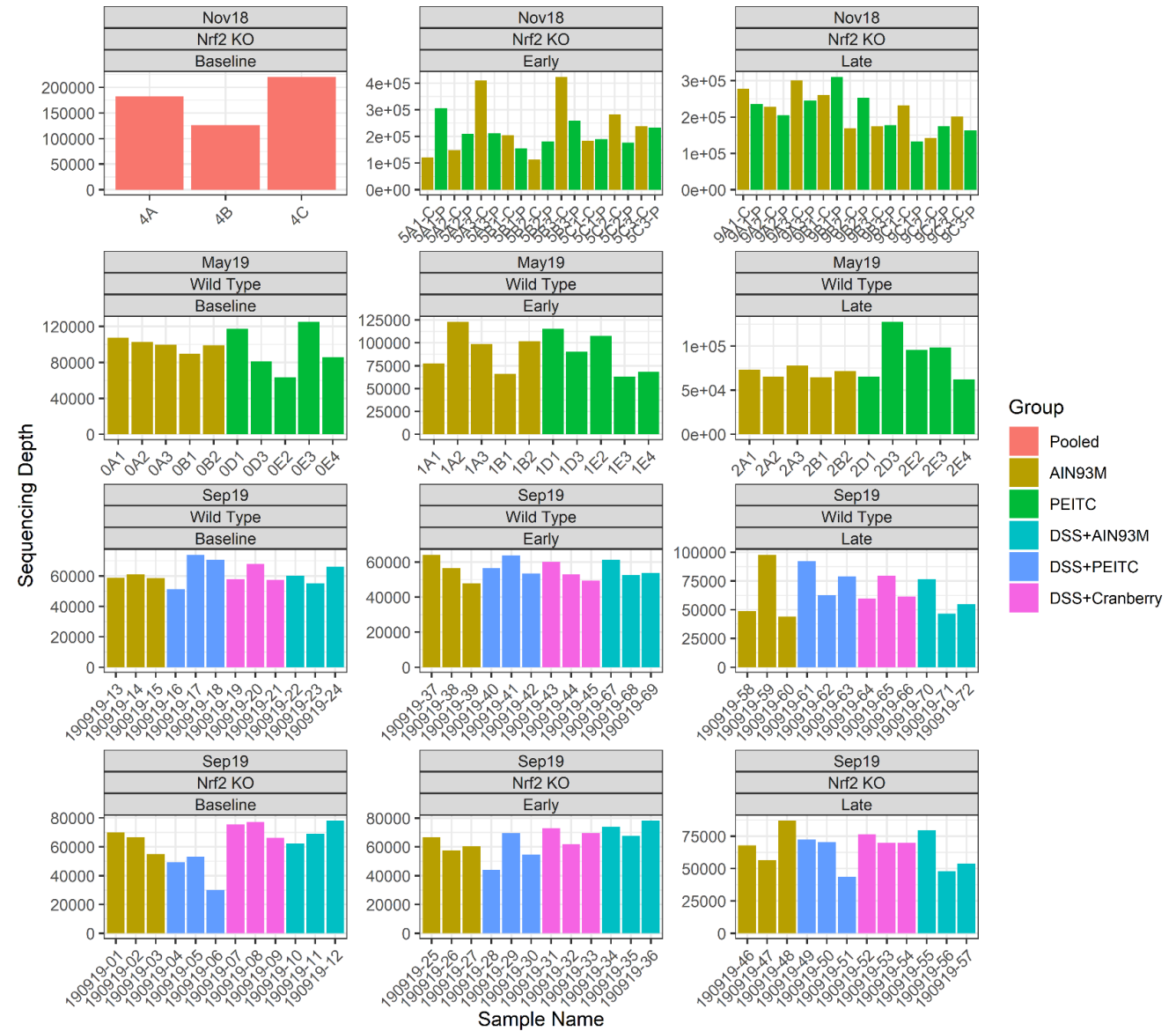
**AIN93M:
Groups 2, 4,
7, 8, 11 and 12**

**AIN93M + 0.05% PEITC Groups 2, 4, 8 and 12
AIN93M + Cranberry: Groups 7 and 11**



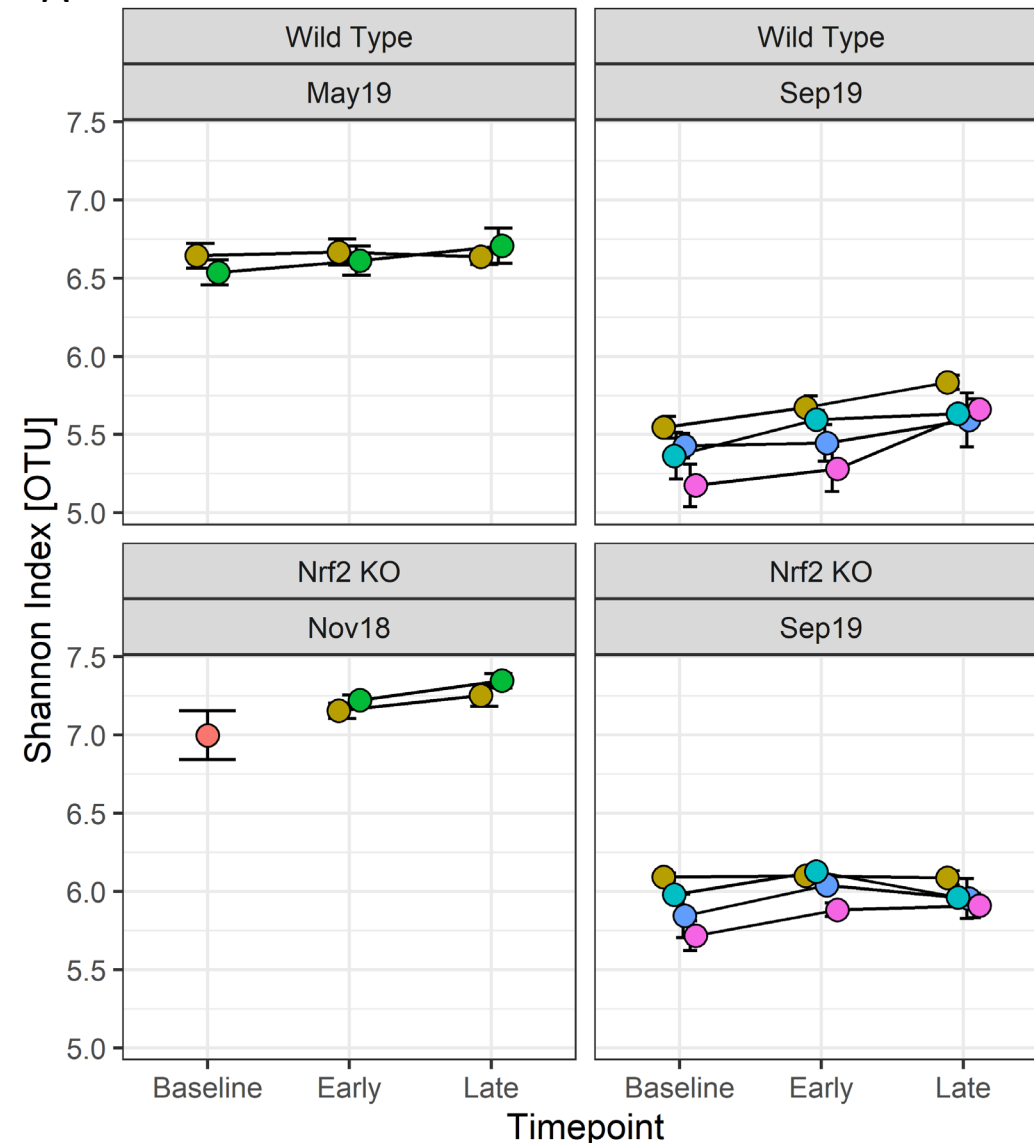
**Gut microbiota
equalization period
(2 weeks)**

Figure 1: Experimental design. Mice fecal samples for the 16S sequencing were collected individually at 3 timepoints – at the end of the 2-week equalization period (Week 0), at an early timepoint (Week 1) and at a late timepoint (Week 4 or Week 8). Samples used for metabolite analysis were collected at an early and a late timepoints (Weeks 2 and Week 6 respectively).

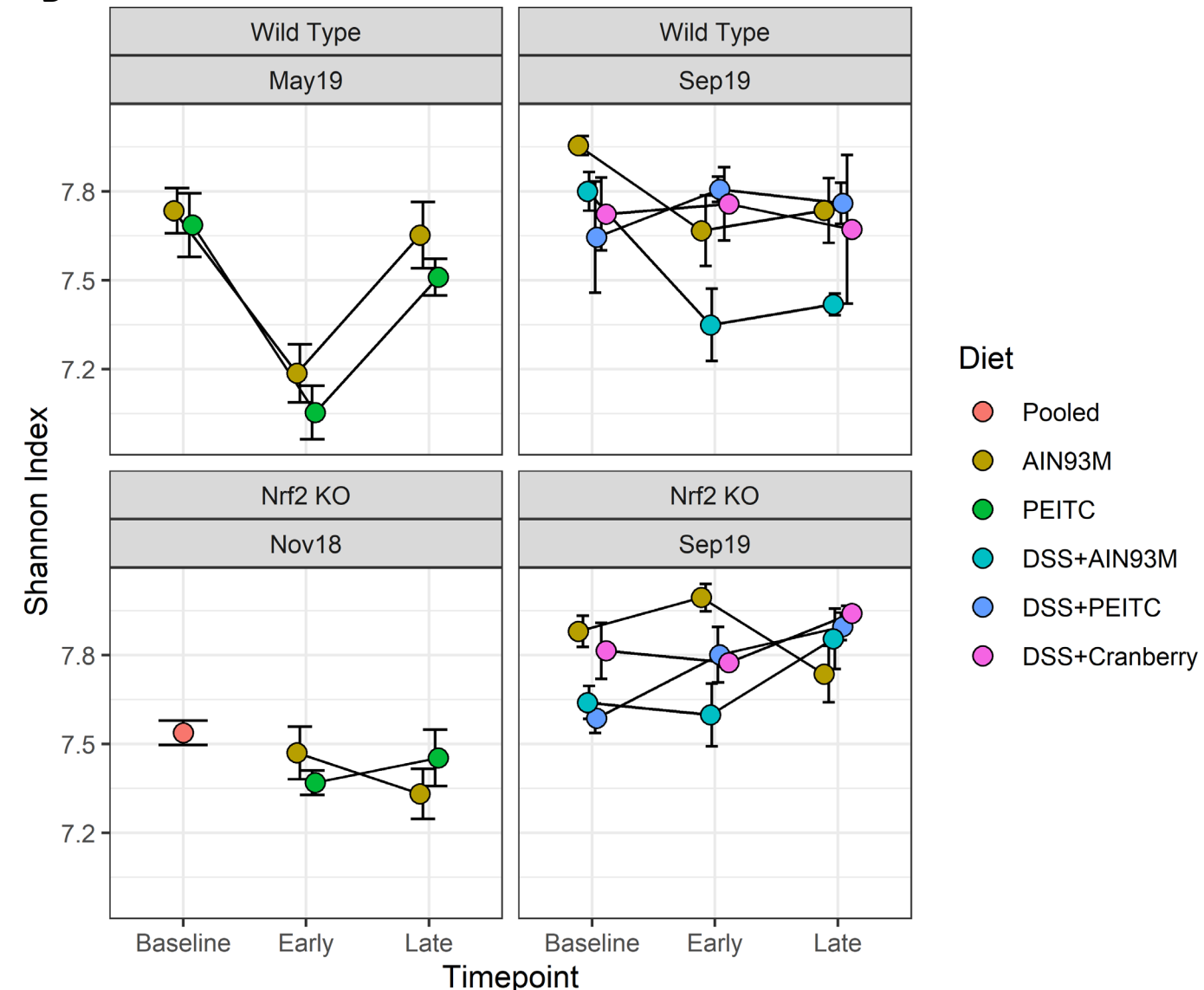


Supplemental Figure 1: 16S sequencing depth (total number of hits per sample).

A

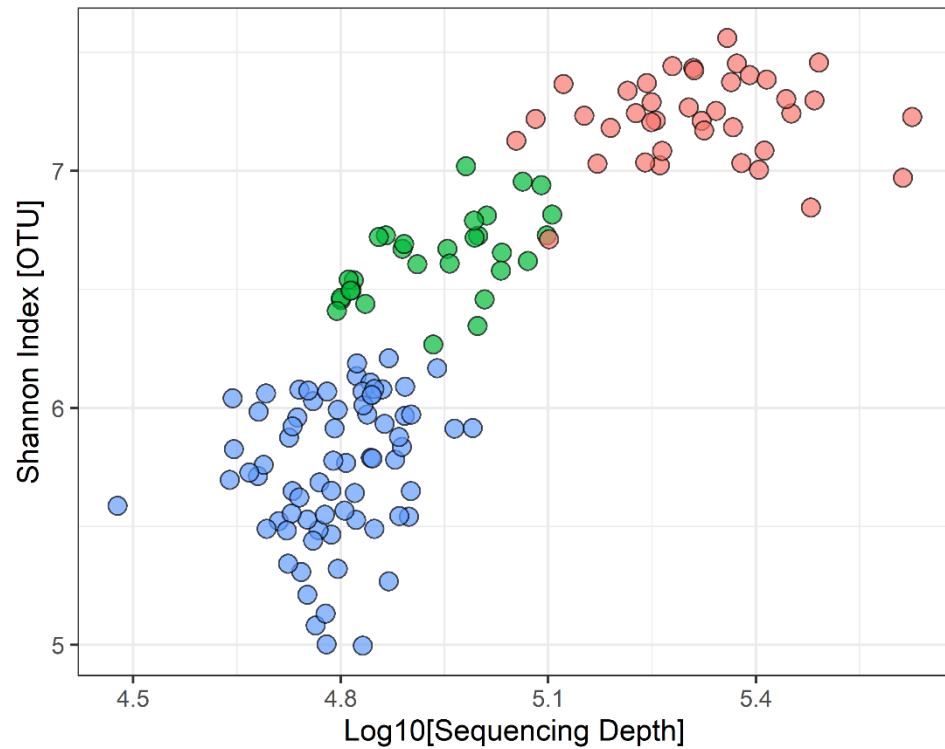
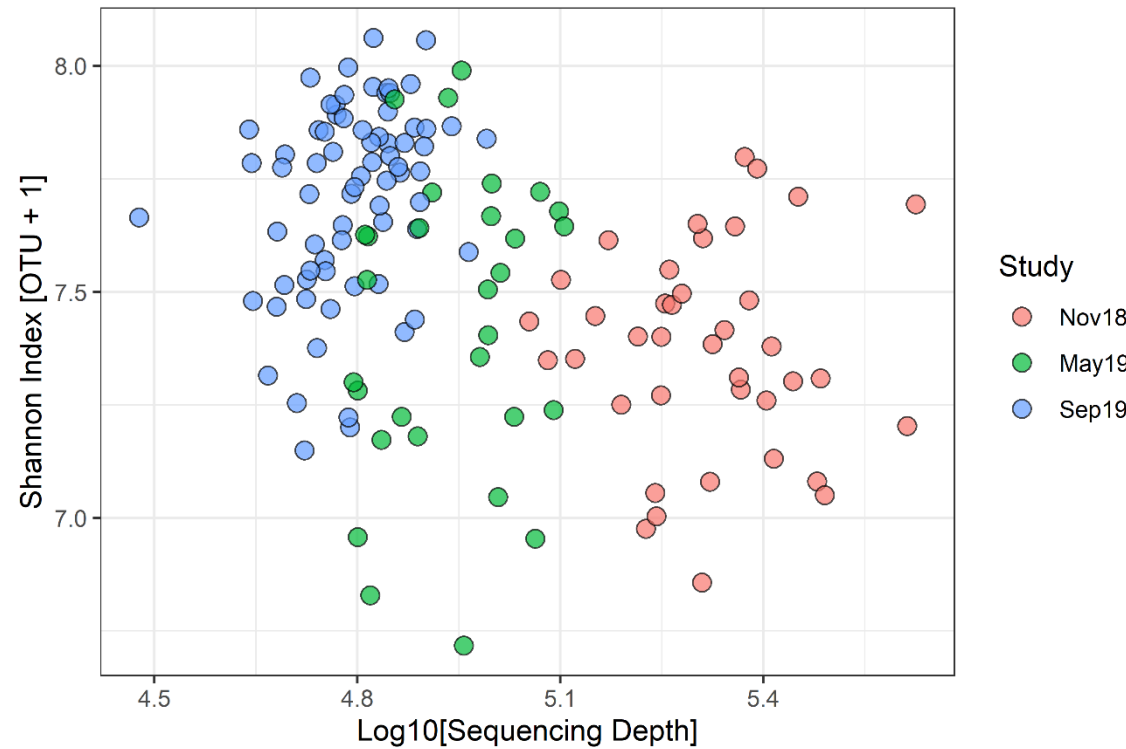


B

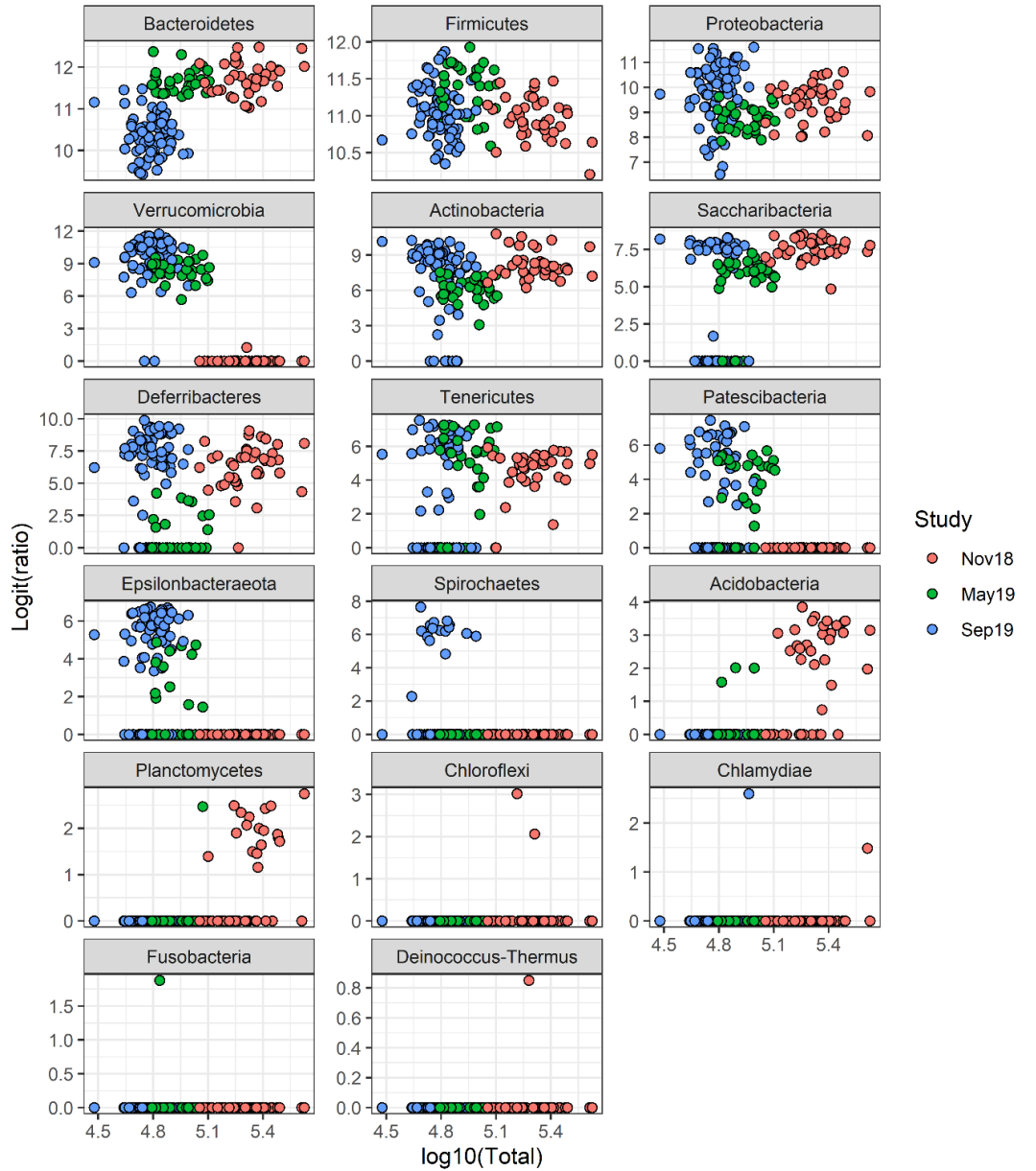


- Diet
- Pooled
 - AIN93M
 - PEITC
 - DSS+AIN93M
 - DSS+PEITC
 - DSS+Cranberry

Figure 2: Alpha diversity measured by Shannon index. (A) Averages of Shannon indices calculated on raw OTU numbers and (B) on corrected OTU numbers (OTU+1).

A**B**

Supplemental Figure 2: Shannon index vs. sequencing depth.



Supplemental Figure 3: logit of the relative abundance of Phylum vs. sequencing depth.

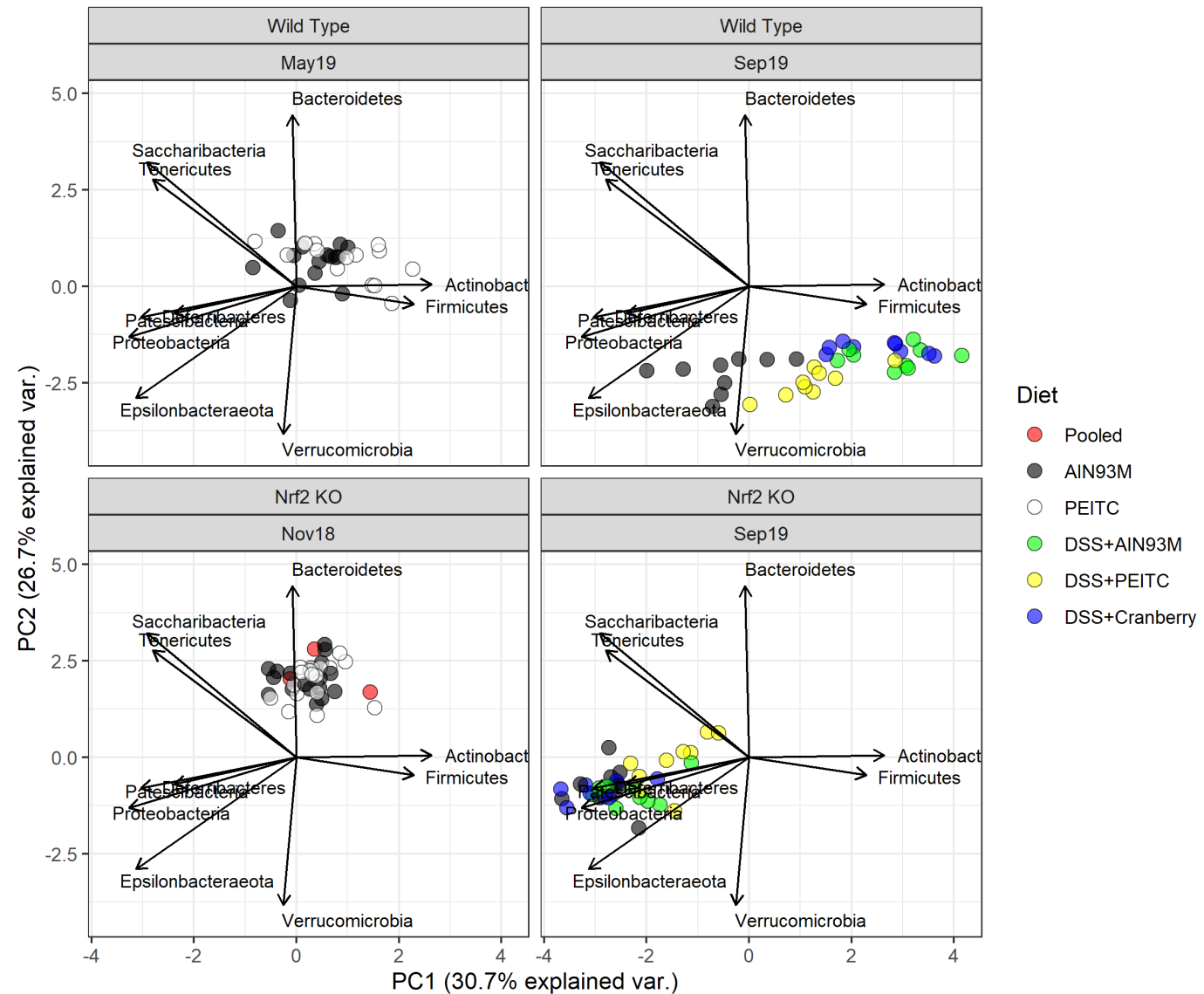


Figure 4: Biplot of logit relative abundance of Phylum

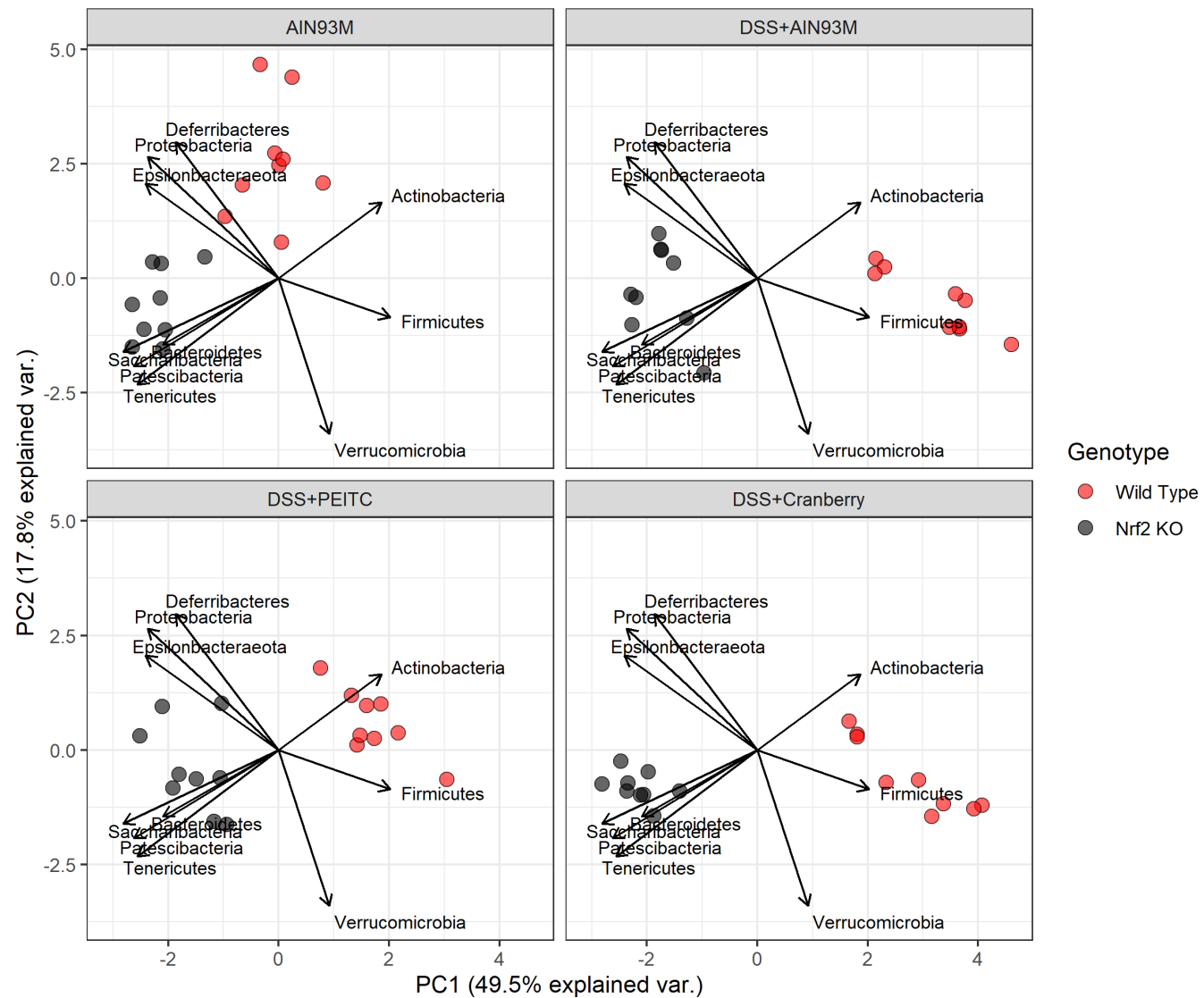


Figure 5: biplot of logit relative abundance of Phylum in Exp03 only

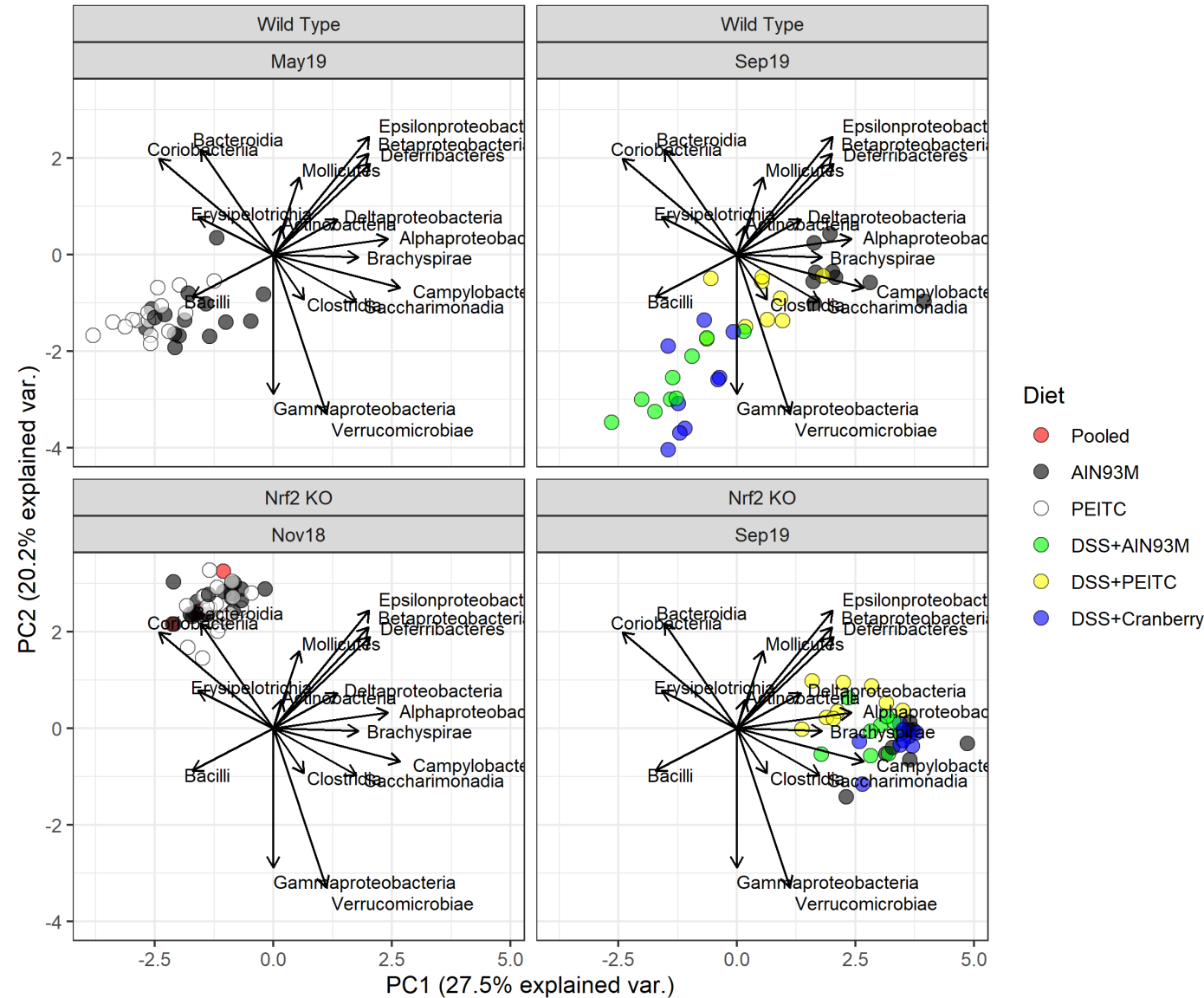


Figure 6: Biplot of logit relative abundance of bacterial classes

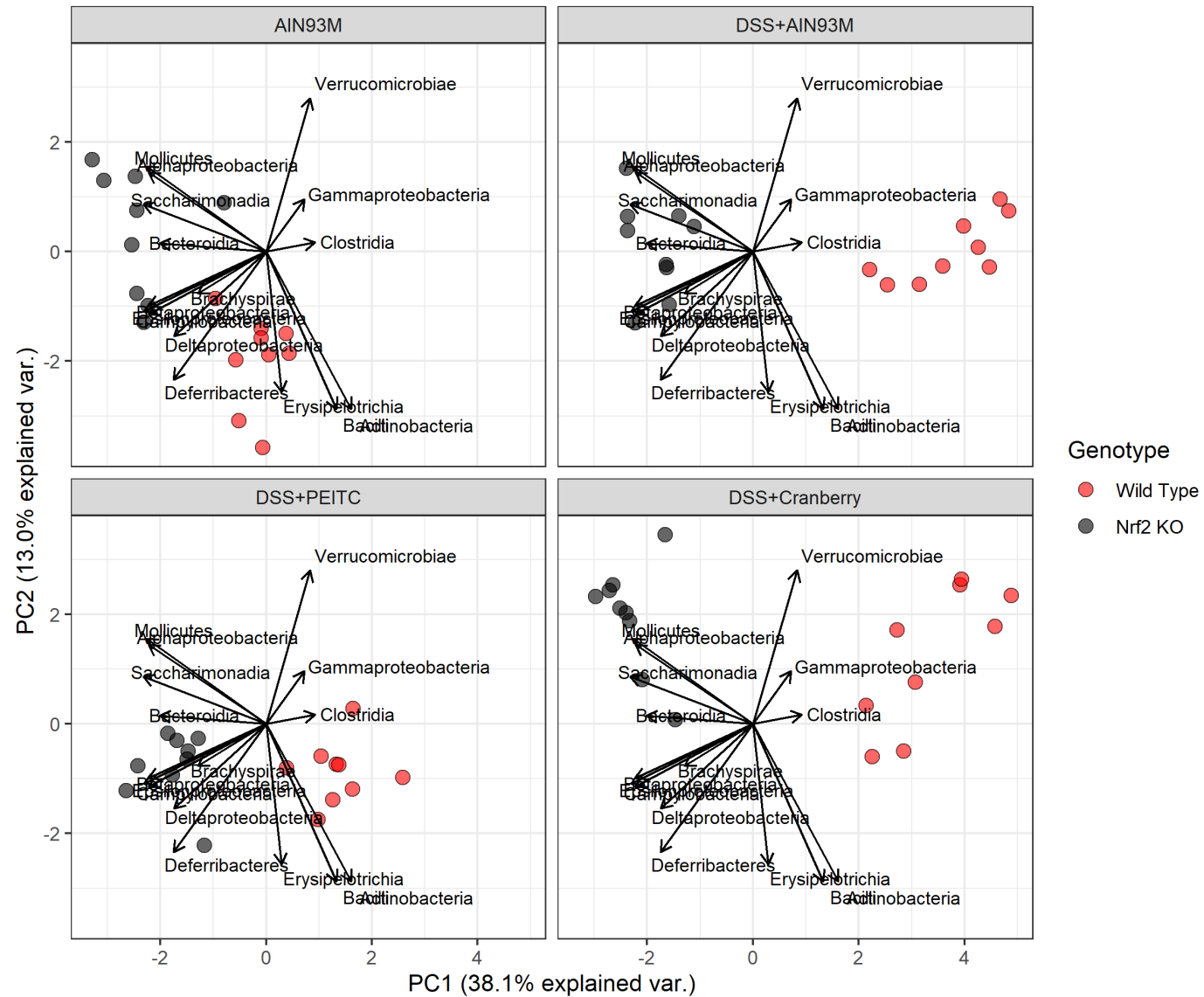


Figure 7: biplot of logit relative abundance of bacterial classes in Exp03 only

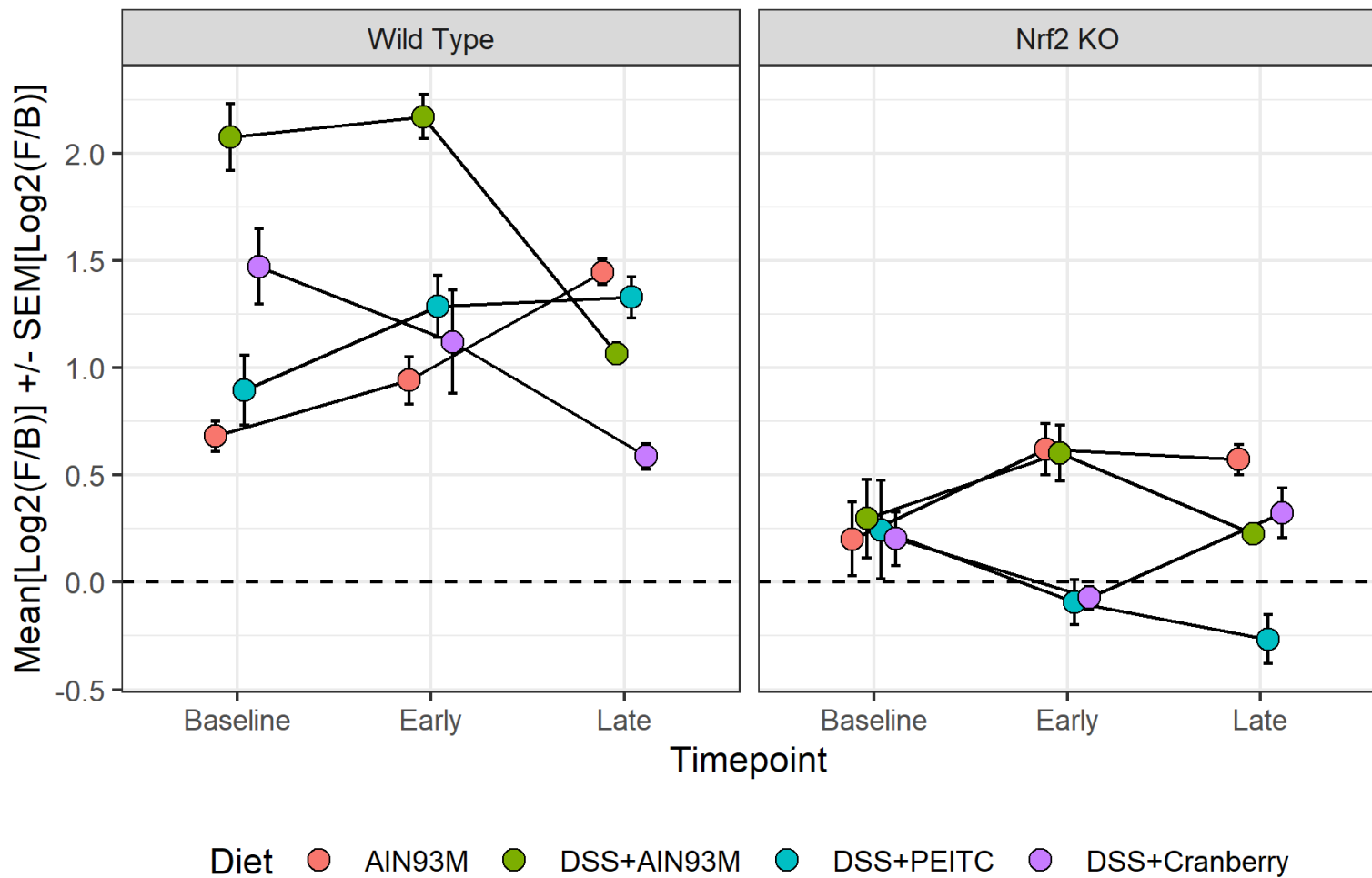


Figure 8: Means of log2 F/B ratios by genotype and diet over time. The bars represent standard errors of log2(F/B) ratios.

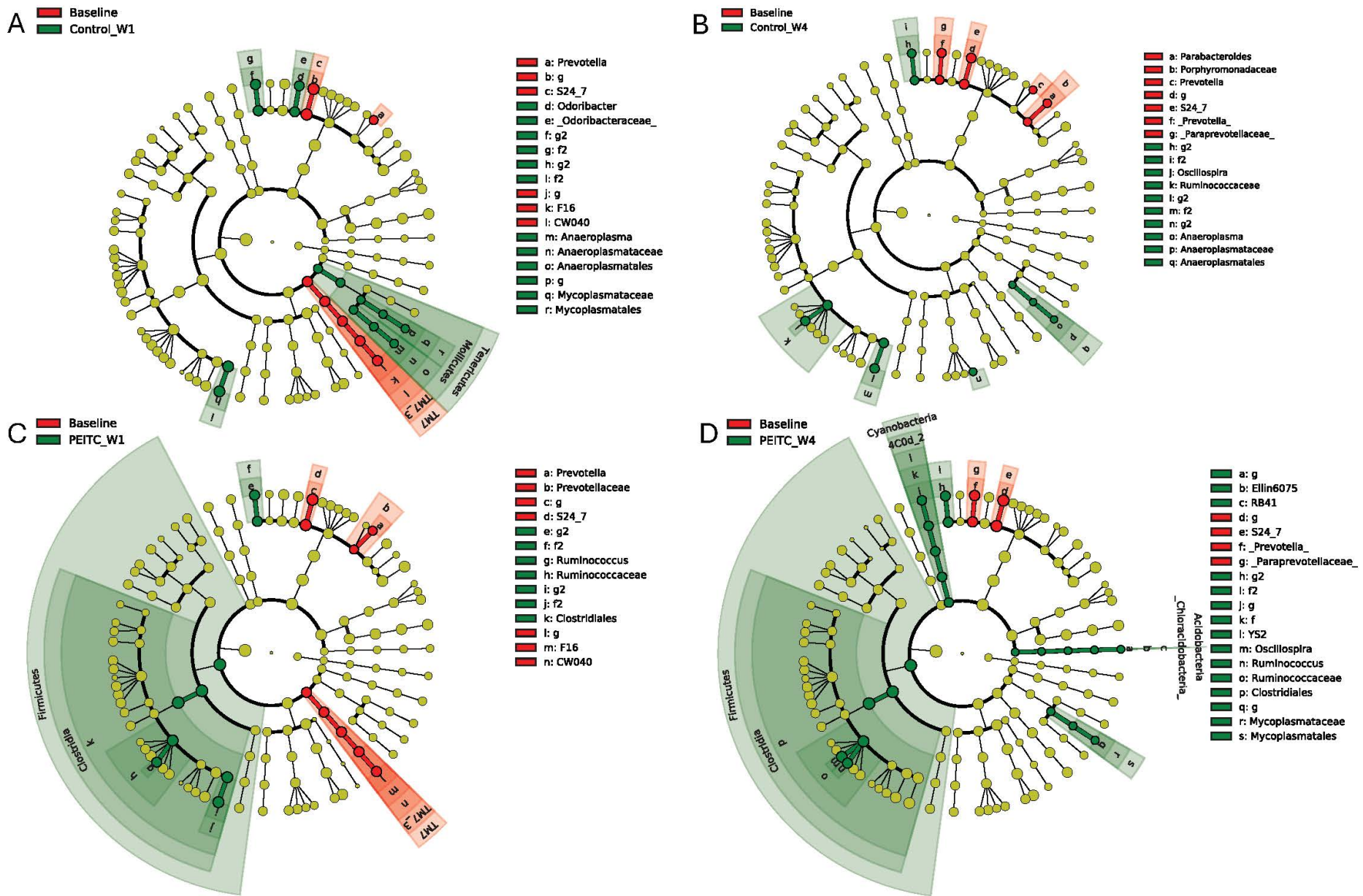
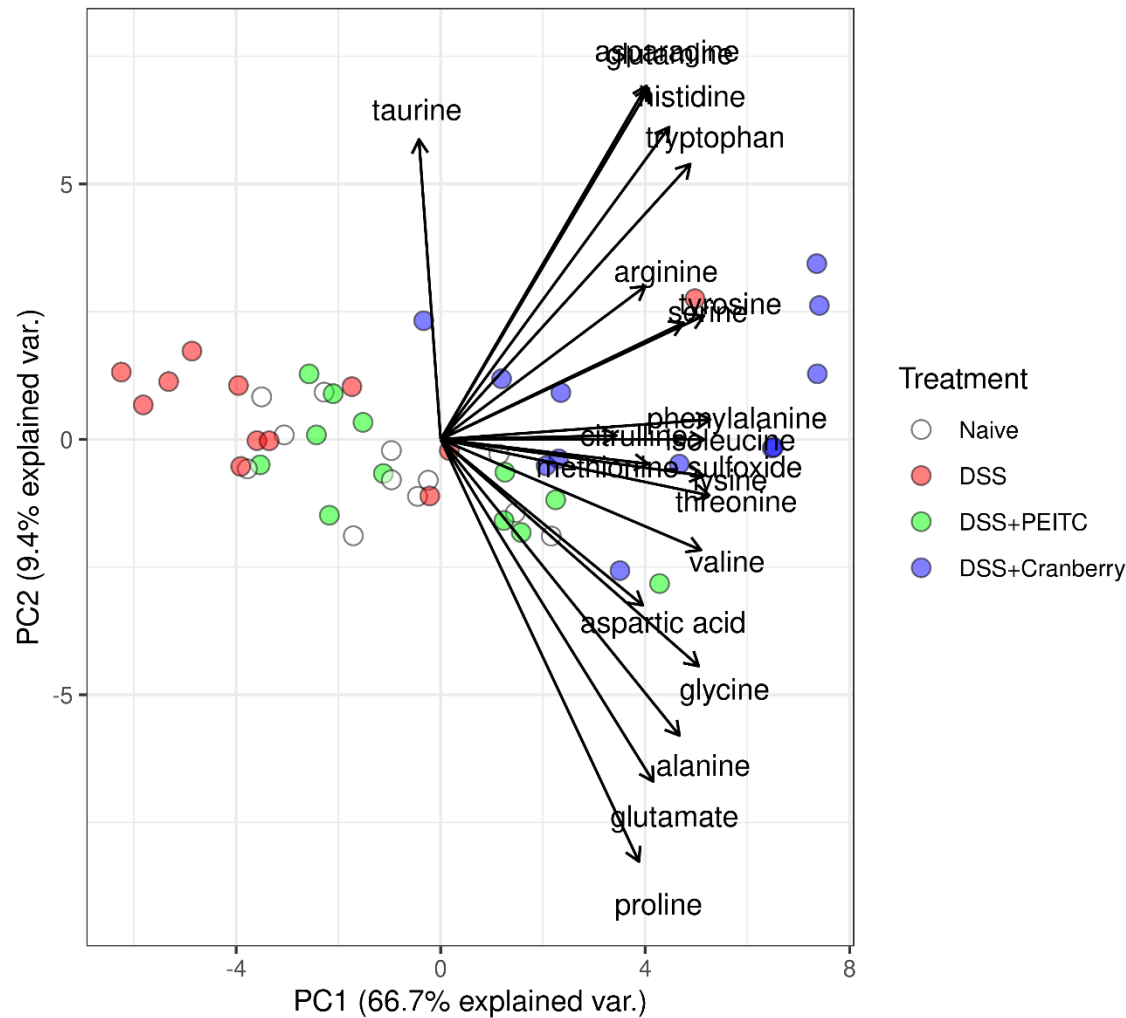


Figure 9: Linear discriminant analysis Effect Size (LEfSe) analysis of aging and PEITC dietary additives effect.

A

Biplot of Aminoacids



B

Biplot of Bile Acids

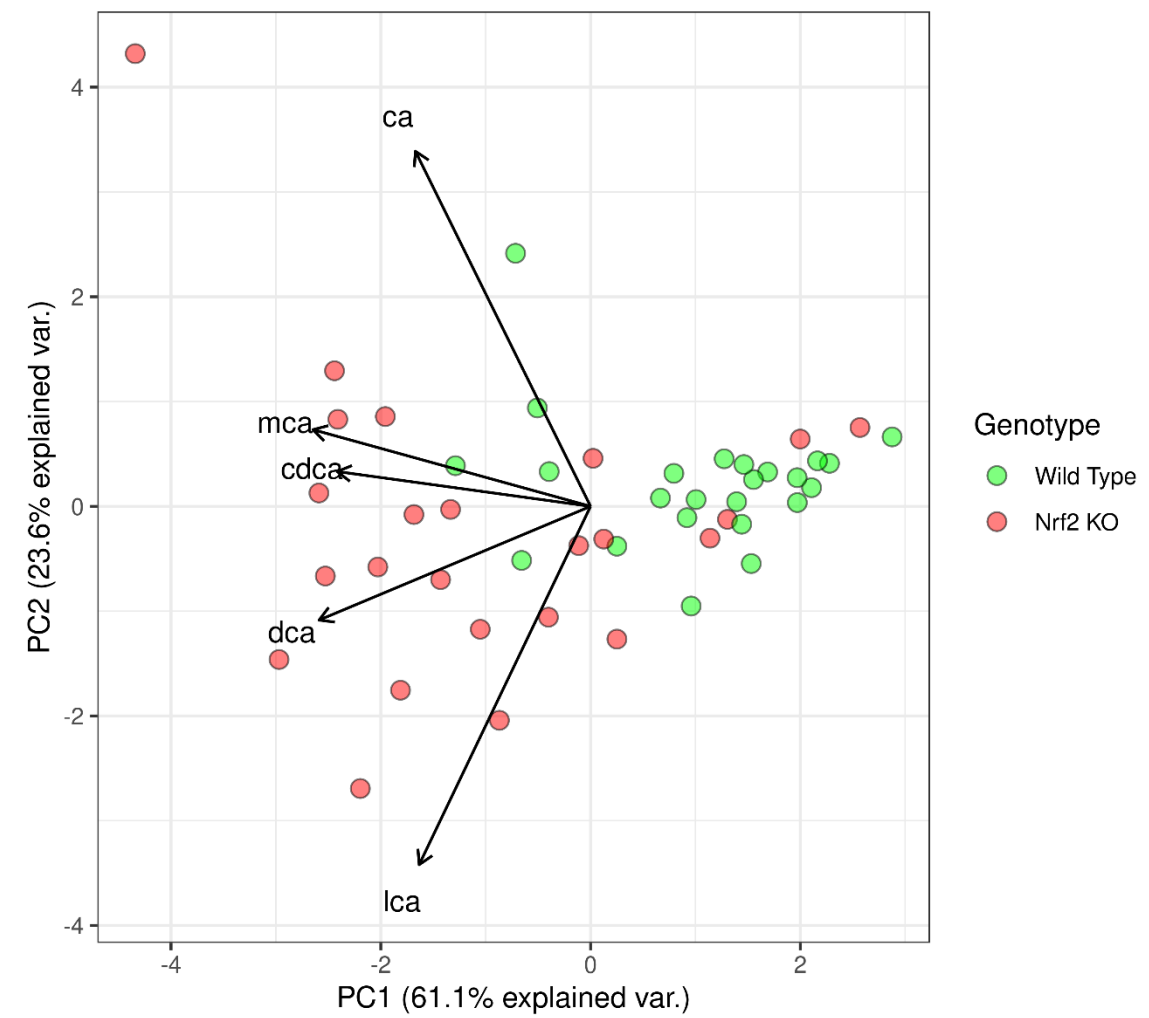


Figure 10: Biplots of amino acids by diet (A) and bile acids by genotype (B).

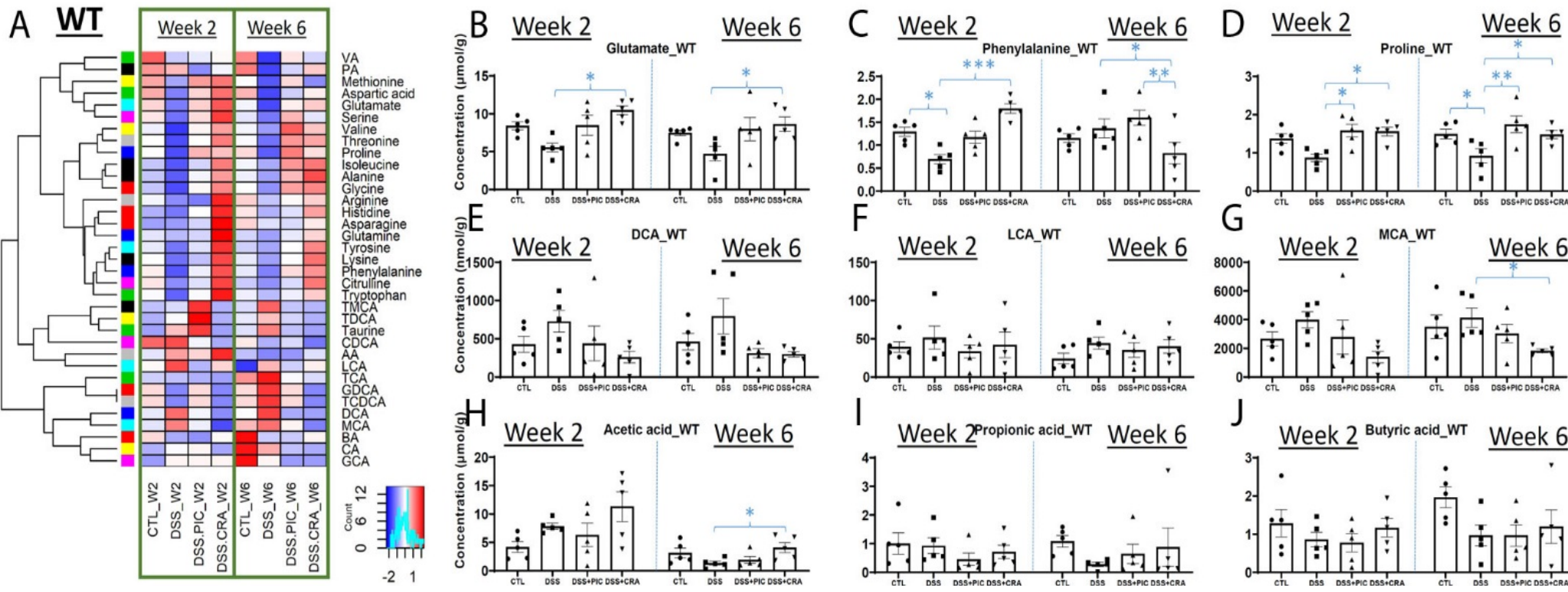


Figure 11: Effects of DSS, PEITC and cranberry cotreatments on fecal metabolome of WT mice. Fecal samples collected at week 2 and 6 of 4 treatments, including control (CTL), DSS, DSS+PEITC (DSS+PIC), and DSS+cranberry (DSS+CRA), were analyzed by 4 LC-MS methods (143). The concentrations of amino acids, bile acids, and SCFA were quantified. (A) A heatmap on the distribution of amino acids, bile acids and SCFA in fecal samples from 4 treatments. (B-D) Concentrations of major amino acids, including glutamate, phenylalanine, and proline. (E-G) Concentrations of major bile acids, including DCA, LCA, and MCA. (H-J) Concentrations of major SCFA, including acetic acid (AA), propionic acid (PA), and butyric acid (BA).

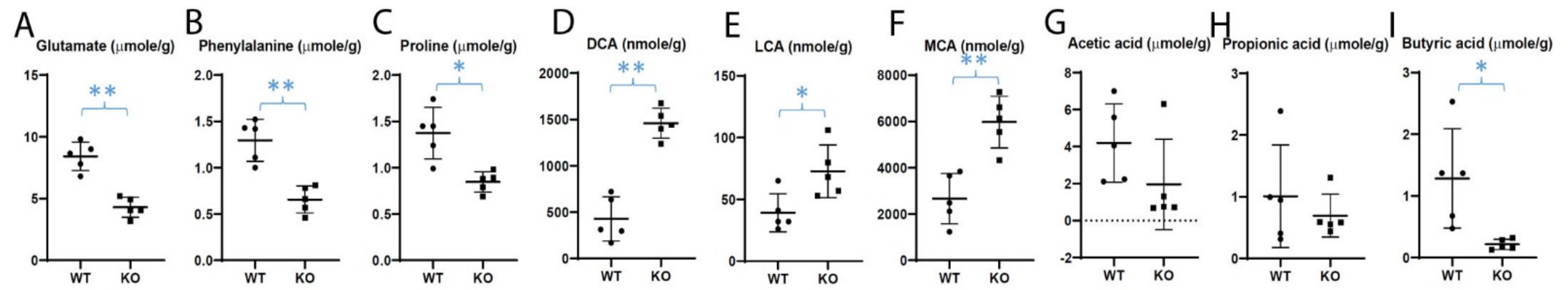


Figure 12: Differences in fecal metabolite profile between WT and Nrf2-null (KO) mice. The concentrations of amino acids, bile acids, and SCFA were quantified in the fecal samples from untreated WT and KO mice (143). (A-C) Concentrations of glutamate, phenylalanine, and proline. (D-F) Concentrations of major bile acids. (G-I) Concentrations of major SCFA.

| Forward Primer | Reverse Primer |
|--------------------|----------------------|
| 515F (Parada) | 806R (Apprill) |
| GTGYCAGCMGCCGCGTAA | GGACTACNVGGGTWTCTAAT |

Supplemental Table 1: V4 primer sequence used for 16s RNA sequencing library preparation

| Kingdom | Experiment 1: Nrf2 KO Mice | Experiment 2: WT Mice | Experiment 3: WT and Nrf2 KO | Combined |
|-----------|-------------------------------|--------------------------|------------------------------------|-----------------|
| Bacteria | 10,197 (94.78%) | 7,994 (98.34%) | 7,558 (96.07%) | 22,251 (95.73%) |
| Eukaryota | 472 (4.39%) | 116 (1.43%) | 232 (2.95%) | 812 (3.49%) |
| Archaea | 4 (0.04%) | 0 (0%) | 2 (0.03%) | 6 (0.03%) |
| Unknown | 86 (0.80%) | 19 (0.23%) | 75 (0.95%) | 175 (0.75%) |

Table 1: OTU mapping to Kingdoms. Number of OTUs found in each experiment (% total).

| Predicted diet and DSS challenge (PC1+PC2+PC3) | Observed diet and DSS challenge | | | |
|--|---------------------------------|------------|-----------|-----------------|
| | No DSS+AIN93M | DSS+AIN93M | DSS+PEITC | DSS + Cranberry |
| No DSS + AIN93M | 4 | 2 | 1 | 0 |
| DSS + AIN93M | 4 | 8 | 1 | 0 |
| DSS + PEITC | 3 | 1 | 6 | 1 |
| DSS + Cranberry | 1 | 1 | 1 | 11 |

Table 2: multinomial regression predictions of treatment groups by microbial metabolite PCA

| Predicted genotype (PC1) | Observed genotype | |
|--------------------------|-------------------|---------|
| | Wild Type | Nrf2 KO |
| Wild Type | 18 | 6 |
| Nrf2 KO | 8 | 16 |

Table 3: multinomial regression predictions of genotype by microbial metabolite PCA